JOURNAL OF GEOPHYSICAL RESEARCH, VOL. 112, B06308, doi:10.1029/2006JB004687, 2007



# Crustal structure due to collisional and escape tectonics in the Eastern Alps region based on profiles Alp01 and Alp02 from the ALP 2002 seismic experiment

Ewald Brückl,[1] Florian Bleibinhaus,[1,12] Andrej Gosar,[2] Marek Grad,[3] Aleksander Guterch,[4] Pavla Hrubcová,[5] G. Randy Keller,[6] Mariusz Majdański,[3] Franjo Šumanovac,[7] Timo Tiira,[8] Jukka Yliniemi,[9] Endre Hegedűs,[10] and Hans Thybo[11]

Received 9 August 2006; revised 17 February 2007; accepted 8 March 2007; published 26 June 2007.

[1] Alp01 and Alp02 are the longest profiles recorded during ALP 2002, a large international seismic refraction and wide-angle reflection experiment undertaken in the Eastern Alps in 2002. Alp01 crosses the Alpine orogen from north to south, thus providing a cross section mainly affected by the collision between Europe and the Adriatic microplate. Alp02 extends from the Eastern Alps to the Pannonian basin, supplying evidence on the relation between Alpine crustal structure and tectonic escape to the Pannonian basin. During this experiment, 363 single-channel recorders were deployed along these profiles with an average spacing of 3.2 km. Recordings from 20 inline shots were used in this study. Two-dimensional forward modeling using interactive ray-tracing techniques produced detailed *P* wave velocity models that contain many features of tectonic significance. Along Alp01, the European Moho dips generally to the south and reaches a maximum depth of 47 km below the transition from the Eastern to the Southern Alps. The Adriatic Moho continues further south at a significantly shallower depth. Moho topography and a prominent south-dipping mantle reflector in the Alpine area support the idea of southward subduction of the European lithosphere below the Adriatic microplate. The most prominent tectonic feature on the Alp02 profile is a vertical step of the Moho at the transition between the Alpine and Pannonian domains, suggesting the existence of a separate Pannonian plate fragment. The development of the Pannonian fragment is interpreted to be a consequence of crustal thinning due to tectonic escape from the Alpine collision area to the Pannonian basin.

**Citation:** Brückl, E., et al. (2007), Crustal structure due to collisional and escape tectonics in the Eastern Alps region based on profiles Alp01 and Alp02 from the ALP 2002 seismic experiment, *J. Geophys. Res.*, *112*, B06308, doi:10.1029/2006JB004687.

## 1. Introduction

[2] From 1997 to 2003, central Europe was covered by a series of large active source seismic refraction and wide-angle reflection (WAR/R) experiments in order to obtain better knowledge of the structure and properties of the crust and the upper mantle [*Guterch et al.*, 2003a]. ALP 2002 was one of these experiments (Figure 1), and it was designed to build on the earlier POLONAISE'97 and CELEBRATION 2000 efforts [*Guterch et al.*, 1999, 2003b] and to provide comprehensive seismic coverage in the Eastern Alps. The area spanned by ALP 2002 is large and extends from the Bohemian massif to the north, across the Molasse basin, the Eastern and Southern Alps to the Dinarides in the south, and the Pannonian basin in the southeast (Figures 1 and 2a). The main ALP 2002 effort was undertaken in July 2002 when about 1000 seismic stations were deployed along 13 lines with a total length of about 4300 km to record the seismic waves generated by 38 shots [*Brückl et al.*, 2003].

[3] Most elements of the present-day crustal structure are the result of tectonic events since the opening of the Atlantic Ocean in Jurassic time. The strike-slip movement of Africa with respect to Europe was replaced by convergence between Europe and Africa in the Cretaceous leading to a first phase of

[1] Institute of Geodesy and Geophysics, Vienna University of Technology, Vienna, Austria.
[2] Environmental Agency of Slovenia and Faculty of Natural Sciences and Engineering, University of Ljubljana, Ljubljana, Slovenia.
[3] Institute of Geophysics, University of Warsaw, Warsaw, Poland.
[4] Institute of Geophysics, Polish Academy of Sciences, Warsaw, Poland.
[5] Geophysical Institute, Academy of Sciences of the Czech Republic, Prague, Czech Republic.


0148-0227/07/2006JB004687$09.00

[6] Department of Geological Sciences, University of Texas at El Paso, El Paso, USA.
[7] Faculty of Mining, Geology and Petroleum Engineering, University of Zagreb, Zagreb, Croatia.
[8] Institute of Seismology, University of Helsinki, Helsinki, Finland.
[9] Sodankylä Geophysical Observatory, University of Oulu, Oulu, Finland.
[10] Eötvös Loránd Geophysical Institute, Budapest, Hungary.
[11] Geological Institute, University of Copenhagen, Copenhagen, Denmark.
[12] Now at Department of Earth and Environmental Sciences, University of Munich, Munich, Germany.

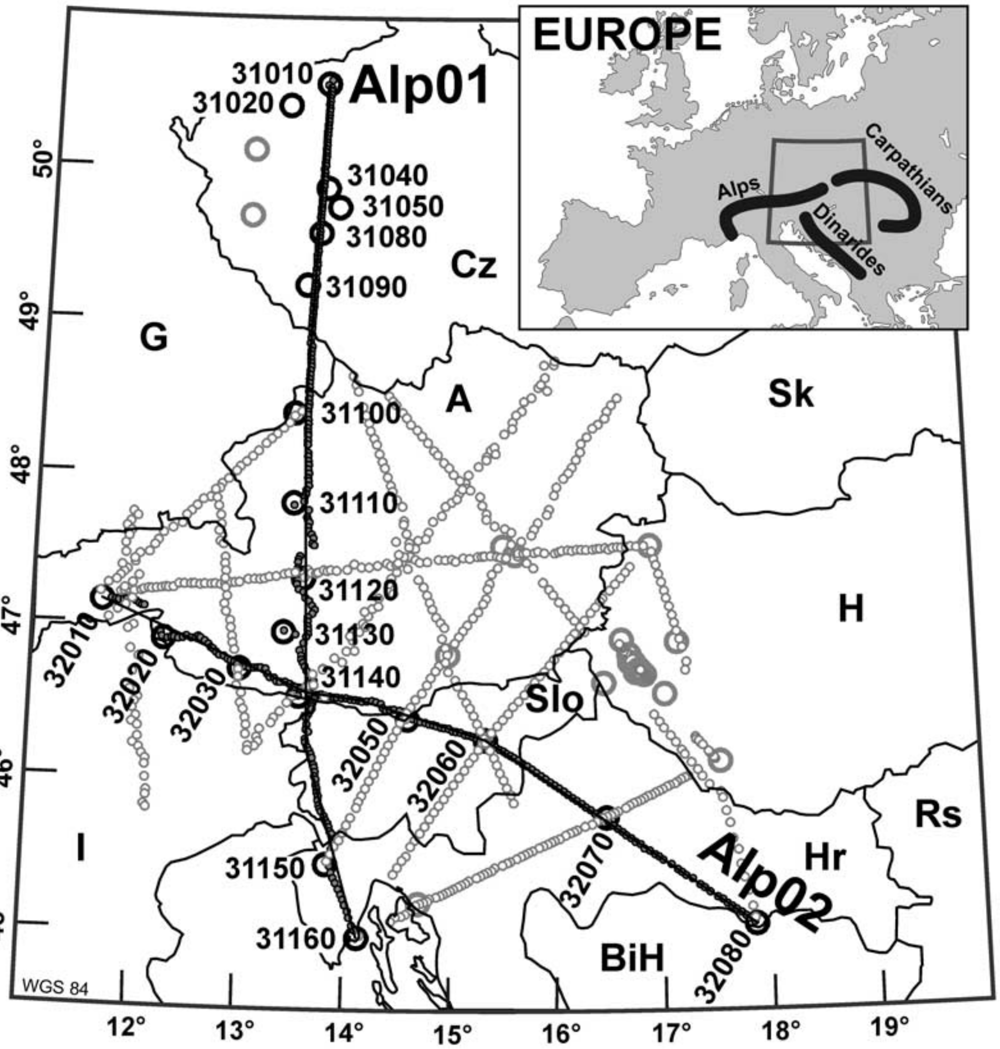


**Figure 1.** Field layout of the ALP 2002 seismic experiment; larger circles are shot locations, smaller circles are receiver locations; shots and receivers on Alp01 and Alp02 are black, others grey; heavy black lines in inset are axes of mountain ranges. Country abbreviations are in bold characters (A, Austria; BiH, Bosnia and Herzegovina; Cz, Czech Republic; G, Germany; H, Hungary; Hr, Croatia; I, Italy; Rs, Republic of Serbia; Slo, Slovenia; Sk, Slovakia).

Alpine orogenic activity [*Schmid et al.*, 2004]. In the Oligocene, the closure of the Alpine ocean basins lead to the collision of the Adriatic microplate (subplate of Africa) with the European platform, causing a second phase of Alpine orogenic activity. Thereafter, in the late Oligocene and early Miocene, roll back of the Carpathian subduction zone generated the Pannonian basin [*Royden et al.*, 1983; *Peresson and Decker*, 1997]. The ongoing movement of Adria toward Europe also formed the Dinaridic orogen. Since the late Oligocene and early Miocene, the Eastern Alps have reacted to the ongoing compression between the Bohemian promontory of the European platform to the north and the indenting Adriatic microplate to the south by tectonic extrusion/escape to the unconstrained eastern margin represented by the Pannonian basin [*Ratschbacher et al.*, 1991].

[4] The Alps, specifically the Eastern Alps and their surroundings, have been a classical target of geophysical investigations and interpretations. Examples of vintage profiles include the Alpine longitudinal profile (ALP'75) that crossed the ALP 2002 from west to east [*Alpine Explosion Seismology Group*, 1976] and the TRANSALP seismic transect [*TRANSALP Working Group*, 2002] that provides an important constraint along the western edge of the ALP 2002 area. However, despite these efforts, the crustal structure in the ALP 2002 area is not resolved well enough to answer several fundamental geodynamic questions. One example is the direction of subduction between the Adriatic and European plates. Whereas the interpretation of the crustal structure along TRANSALP indicates subduction of the European plate below the Adriatic indenter [*TRANSALP Working Group*, 2002], teleseismic tomography indicates the opposite direction of subduction [*Lippitsch et al.*, 2003; *Schmid et al.*, 2004]. The extent and processes of crustal thickening or thinning are a general issue. A particular point is the step in the Moho depth from 50 to 35 km that occurs at about 14.5°E longitude in the far Eastern Alps along the ALP'75 profile [*Yan and Mechie*, 1989]. This step to a

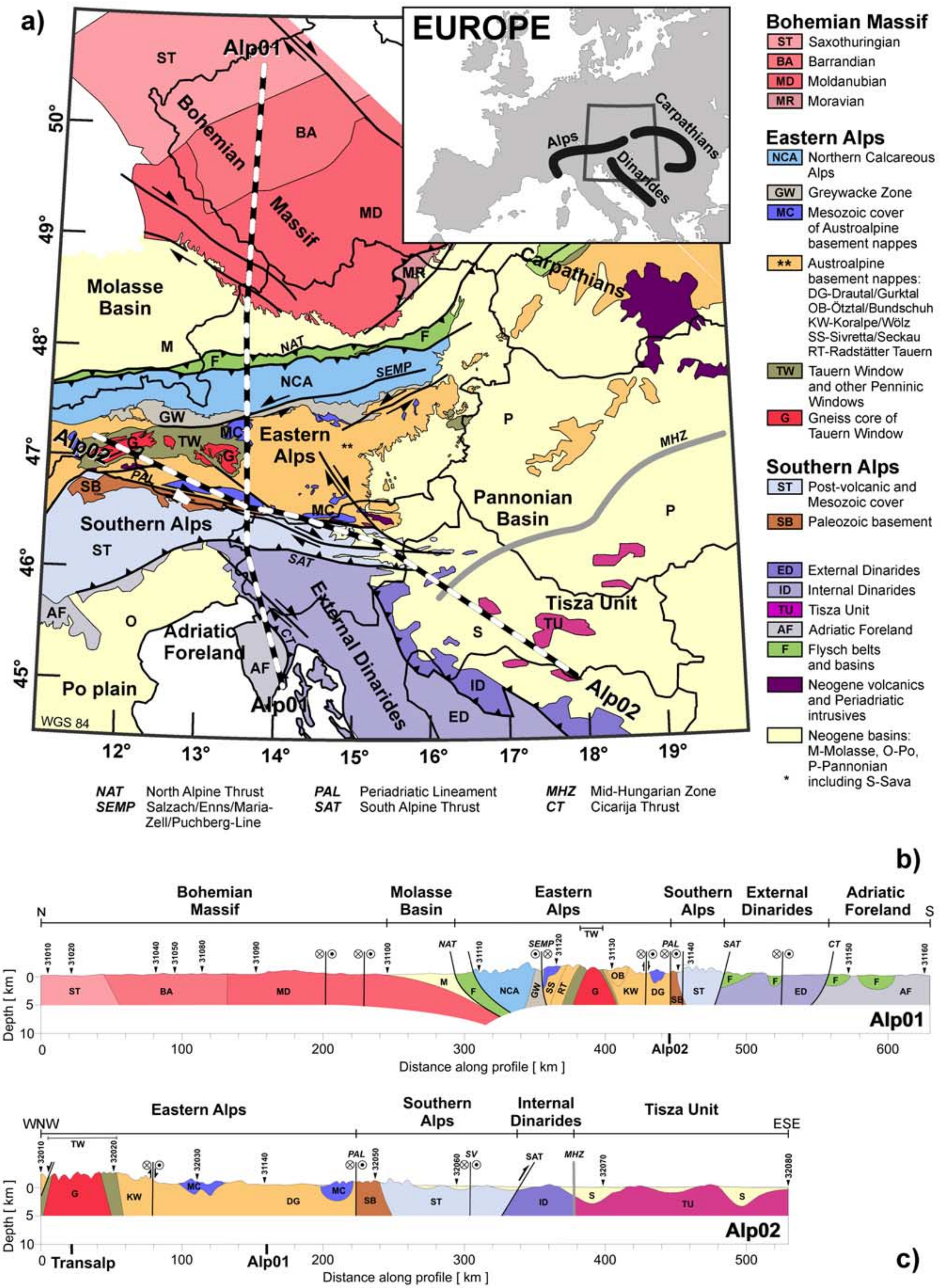

a)
EUROPE
Alps
Carpathians
Dinarides
Bohemian Massif
ST Saxothuringian
BA Barrandian
MD Moldanubian
MR Moravian
Eastern Alps
NCA Northern Calcareous Alps
GW Greywacke Zone
MC Mesozoic cover of Austroalpine basement nappes
** Austroalpine basement nappes: DG-Drautal/Gurktal OB-Ötztal/Bundschuh KW-Koralpe/Wölz SS-Sivretta/Seckau RT-Radstätter Tauern
TW Tauern Window and other Penninic Windows
G Gneiss core of Tauern Window
Southern Alps
ST Post-volcanic and Mesozoic cover
SB Paleozoic basement
ED External Dinarides
ID Internal Dinarides
TU Tisza Unit
AF Adriatic Foreland
F Flysch belts and basins
Neogene volcanics and Periadriatic intrusives
Neogene basins: M-Molasse, O-Po, P-Pannonian
* including S-Sava
NAT North Alpine Thrust
SEMP Salzach/Enns/Maria-Zell/Puchberg-Line
PAL Periadriatic Lineament
SAT South Alpine Thrust
MHZ Mid-Hungarian Zone
CT Cicarija Thrust
Molasse Basin
Southern Alps
Adriatic Foreland
Po plain
Pannonian Basin
Tisza Unit
External Dinarides
WGS 84
Alp01
Alp02
b)
Bohemian Massif
Molasse Basin
Eastern Alps
Southern Alps
External Dinarides
Adriatic Foreland
Depth [ km ]
Distance along profile [ km ]
c)
Eastern Alps
Southern Alps
Internal Dinarides
Tisza Unit
WNW
ESE
Transalp


**Figure 2**

shallower Moho to the east was confirmed by the studies of *Scarascia and Cassinis* [1997] and was interpreted as the boundary between two Moho "patches." However, the question whether this feature is mainly a consequence of extrusion/escape tectonics or follows from the interaction of the Adriatic indenter with Europe during the collision process cannot be decided on the basis of these results. A further issue is the continuation of large-scale faults like the Peri-Adriatic line/lineament (PAL) in the deeper crust (Figure 2a). The goals of the ALP 2002 project included supplying answers to these and similar questions by two-dimensional forward modeling of individual profiles and by a three-dimensional approach using stacking techniques [*Behm*, 2006; *Behm et al.*, 2007]. In this paper, we concentrate on interactive modeling by ray tracing along the two major ALP 2002 profiles, Alp01 and Alp02.

## 2. Previous Work

[5] The exploration of the lithosphere of the Eastern Alps and our area of interest by WAR/R experiments started around the Eschenlohe quarry 40 years ago. Seismic lines spread out from this shotpoint across the Alps to the shotpoints Lago Lagorai and Trieste [*Giese and Prodehl*, 1976]. The Alpine longitudinal profile (ALP'75) began in the Western Alps and extended along the axis of the Alps to the Pannonian basin. Several authors and interpretation teams [*Alpine Explosion Seismology Group*, 1976; *Miller et al.*, 1977; *Aric and Gutdeutsch*, 1987; *Yan and Mechie*, 1989] generated seismic models from the ALP'75 data using ray-tracing methods and amplitude analysis. ALP'75 and other lines from Lago Lagorai to the east and between Eschenlohe and Trieste were reinterpreted by *Scarascia and Cassinis* [1997] applying the same methodology and interpretation principles to all data. Information about the crust and especially the Moho depth in the Czech Republic came from the international profiles VI and VII [*Beránek and Zounková*, 1977; *Beránek and Zátopek*, 1981]. The deep seismic reflection profile HR9 supplied detailed information on the crustal structure and Moho in the area of our interest [*Tomek et al.*, 1997; *Vrána and Štědrá*, 1998]. In Slovenia and Croatia, the refraction lines Pula-Maribor [*Joksović and Andrić*, 1983] and Dugiotok-Virovitica [*Joksović and Andrić*, 1982] supplied information on the crustal structure and Moho depth. Most of these results concerning the crustal structure in the ALP 2002 area were used by *Dèzes and Ziegler* [2001] to compile a map of the depth of the Moho. The modern TRANSALP project crossed the Eastern Alps from Munich to Venice. Steep and wide-angle reflection techniques, diving wave tomography, and receiver function inversions of passive monitoring data have been combined to provide an integrated lithospheric structural interpretation [*Lüschen et al.*, 2004]. By design, some ALP 2002 profiles overlapped with TRANSALP and the eastern portion of CELEBRATION 2000, and the results from these projects also provide information on the crustal structure in the ALP 2002 area of interest [*Hrubcová et al.*, 2005; *Majdański et al.*, 2006; *Grad et al.*, 2006; *Bleibinhaus et al.*, 2006].

## 3. Experiment Design

[6] The field layout of the ALP 2002 experiment is shown in Figure 1. Alp01 trends N-S and extends from the Czech Republic to the Istria Peninsula (Figures 1 and 2a). A total of 212 single-channel recorders were deployed over this profile whose length is 633 km. The second profile, Alp02, trends WNW-ESE and begins in the central part of the Eastern Alps and extends to the SSE across the Southern Alps, the Inner Dinarides, and ends in the Pannonian basin. A total of 151 single-channel recorders were deployed over a profile length of 533 km. All recorders were of the Texan (RefTek 125, Refraction Technology, Inc.) type and employed 4.5-Hz vertical geophones.

[7] The sampling rate was 100 Hz, and the recording time was 300 s for each shot. Information on the 20 shots used for the interpretation of Alp01 and Alp02 is compiled in Table 1. Shot 31140 represents the crossing point of Alp01 and Alp02 and was used for the interpretation of both profiles. The standard shooting procedure was to employ 300-kg explosives in five to eight boreholes at 3050-m depth. The shots in the Czech Republic were quarry blasts with charges of up to 10 tons. The timing of the seismic shots was either by automatic shooting at Global Positioning System (GPS)-controlled time or by recording the ignition current. The records were time reduced by 8 km/s reduction velocity and cut to a length of 100 s.

## 4. Tectonic Setting and Geologic Cross Sections

[8] The tectonic provinces, geological units, and major structures traversed by the ALP 2002 experiment area are shown in Figure 2a together with geological cross sections along the Alp01 and Alp02 profiles (Figures 2b and 2c). In order to facilitate our interpretation effort, we compiled these cross sections based mainly on the works of *Schmid et al.* [2004], *Oberhauser* [1980], and *Franke and Żelaźniewicz* [2000]. To the north, Alp01 begins on the Bohemian massif that was accreted to Central Europe in the late Paleozoic. It then crosses the eastern portion of the classic Molasse basin, the Eastern and Southern Alps, and the External Dinarides before ending in the Adriatic foreland. Since Alp01 crosses the Alpine orogen oriented approximately in the direction of maximum compression, it should be dominated by structures generated by collisional processes. Alp02 begins at the western end of the Tauern window where the north-south compression in the Eastern Alps is at its maximum as evidenced by rocks derived from the Penninic Ocean and the underlying European gneissic basement being extruded and exhumed. It extends in ESE direction through the Southern Alps and Dinarides, crossing several dextral transverse faults, until it reaches the Tisza unit of the Pannonian basin. In contrast to the tectonic setting of Alp01, Alp02 should supply evidence on the tectonic extrusion/escape processes of the Eastern

**Figure 2.** (a) Geology and tectonics of the ALP 2002 investigation area; black and white lines denote the locations of the geological cross sections along (b) Alp01 and (c) Alp02; map and cross sections are generalized after the works of *Schmid et al.* [2004], *Oberhauser* [1980], and *Franke and Żelaźniewicz* [2000]; further references are given in the text.

**Table 1.** Information on Seismic Shots on Alp01 and Alp02 (Coordinates in WGS84)[a]

| Profile | Shot | Longitude | Latitude | Profile Distance, km | Lateral Offset, km | UTC Year 2002 | Charge, kg |
|---|---|---|---|---|---|---|---|
| Alp01 | 31010 | 13°42′58″ | 50°34′23″ | 5 | 0 | 185:03:05:00.04 | 400 (Q) |
| | 31020 | 13°19′45″ | 50°25′36″ | 22 | +27 | 185:03:15:01.22 | 10,000 (Q) |
| | 31040 | 13°43′45″ | 49°53′18″ | 81 | −5 | 184:04:00:01.61 | 10,000 (Q) |
| | 31050 | 13°50′60″ | 49°45′53″ | 95 | −14 | 185:18:30:01.42 | 2,000 (Q) |
| | 31080 | 13°40′02″ | 49°35′37″ | 114 | −2 | 184:18:30:02.67 | 2,000 (Q) |
| | 31090 | 13°32′27″ | 49°15′09″ | 152 | +5 | 184:18:00:00.29 | 2,000 (Q) |
| | 31100 | 13°27′10″ | 48°24′38″ | 245 | +7 | 185:02:00:01.59 | 300 |
| | 31110 | 13°27′35″ | 47°49′18″ | 310 | +8 | 185:02:30:04.87 | 300 |
| | 31120 | 13°34′02″ | 47°19′34″ | 365 | +2 | 184:01:59:58.52 | 300 |
| | 31130 | 13°23′23″ | 46°58′26″ | 405 | +16 | 186:02:10:00.13 | 300 |
| | 31140 | 13°32′47″ | 46°33′14″ | 451 | +6 | 186:02:20:00.66 | 300 |
| | 31150 | 13°49′41″ | 45°27′07″ | 572 | +8 | 185:23:05:00.00 | 300 |
| | 31160 | 14°07′56″ | 44°58′16″ | 626 | 0 | 186:04:40:00.00 | 400 |
| Alp02 | 32010 | 11°37′55″ | 47°11′19″ | 0 | 0 | 184:02:30:03.54 | 300 |
| | 32020 | 12°14′44″ | 46°54′57″ | 52 | +8 | 184:02:20:00.53 | 300 |
| | 32030 | 12°58′40″ | 46°43′48″ | 111 | +4 | 184:02:10:01.97 | 300 |
| | 32050 | 14°35′07″ | 46°24′38″ | 158 | +3 | 185:02:20:00.64 | 300 |
| | 31140 | 13°32′47″ | 46°33′14″ | 237 | +5 | 186:02:20:00.66 | 300 |
| | 32060 | 15°19′22″ | 46°16′38″ | 294 | 0 | 183:23:05:00.00 | 300 |
| | 32070 | 16°27′53″ | 45°46′00″ | 398 | −2 | 185:02:40:00.00 | 300 |
| | 32080 | 17°50′40″ | 45°03′38″ | 530 | 0 | 184:02:40:00.01 | 300 |

[a]Lateral offset of shot is positive to the right side of the profile axis; in column "Charge," (Q) means shot in a quarry.

Alps toward the unconstrained margin to the east represented by the Pannonian basin.

### 4.1. Tectonic Setting of the Alp01 Profile

[9] West of 14°–15°E, the Alps are a classic collision orogen [e.g., *Moores and Twiss*, 1995; *Hatcher and Williams*, 1986]. The Alpine accretionary wedge, which includes the Flysch zone, the Northern Calcareous Alps, the Austro-alpine nappes, and their Mesozoic cover, overthrusts the Molasse basin and the Bohemian massif/European platform at the North Alpine thrust (Figures 2a and 2b). The Southern Alps overthrust the Adriatic foreland and the Po Plain to the west and the External and Internal Dinarides to the east along the South Alpine thrust (SAT, Figures 2a–2c). The External Dinarides overthrust the Adriatic foreland along a NW-SE striking thrust fault. The transition from the Eastern to the Southern Alps is characterized by a change from south-dipping to north-dipping thrust faults, and the vergence of folds changes from north to south to produce a bivergent orogen. N-S compression of ~64 km since Early Miocene [*Linzer et al.*, 2002], focal mechanisms in the Southern Alps [*Bressan et al.*, 1998], and continuing convergence and uplift measured by GPS [*Grenerczy and Kenyeres*, 2006] and leveling [*Höggerl*, 1989] provide evidence that collision tectonics is still at work.

[10] In the area of the Bohemian massif, Alp01 (Figures 2a and 2b) crosses a region that experienced successive accretions of terranes to cratonal Europe (Baltica). The accretion of the Saxothuringian, Barrandian, and Moldanubian tectonostratigraphic units took place during the Cadomian and Variscan orogenies late Precambrian and early Carboniferous times [*Dallmeyer et al.*, 1994; *Vrána and Štědrá*, 1998; *Matte*, 2001]. During this tectonism, Moldanubia was intruded by large granitic plutons [*Franke and Żelaźniewicz*, 2000]. At present, the Saxothuringian unit in the north is thrust beneath the Moldanubian unit in the south. A structurally higher unit, the Barrandian, was thrust over both the Saxothuringian and the Moldanubian rocks from the east [*Pitra et al.*, 1999]. The boundary between the Saxothuringian and Barrandian units is covered by Tertiary sediments and volcanic rocks of the Eger rift, which is a Neogene feature characterized by significant Oligocene-Miocene volcanism. Further to the south, the crust of the Bohemian massif dips to the south below the Molasse basin, which represents the northern foreland of the Alps. The geology of the Molasse basin is well known from exploration for hydrocarbons [*Brix and Schultz*, 1993]. Before collision of Europe with the Adriatic microplate in Oligocene, the southern margin of the Bohemian massif was the passive margin of the Penninic (Piedmont-Liguria) Ocean and experienced weakening by normal faulting [*Roeder*, 1977]. At the Northern Alpine thrust (NAT), the Flysch belt was overthrusted onto the Molasse basin. The Flysch belt was in turn overthrust by the Mesozoic Northern Calcareous Alps (NCA) and their Paleozoic base (Greywacke). Together with the Flysch belt, these units form the northern accretionary wedge of the Alpine orogen. To the south, the SEMP (Salzach-Enns-Mariazell-Puchberg) fault represents a prominent sinistral transverse fault that has experienced 60 km of horizontal displacement since Miocene [*Linzer et al.*, 2002]. South of the SEMP fault, the central part of the Eastern Alps consists of a stack of crystalline Upper and Lower Austro-Alpine nappes, their Mesozoic cover, and units of the Tauern window (TW). The Tauern window comprises Penninic nappes and, in the center, even the sub-Penninic granitic gneiss of the European basement has been exhumed from a depth of more than 25 km [*Fügenschuh et al.*, 1977].

[11] The PAL is the boundary between the Eastern Alps and the Southern Alps. Right-lateral movements of about 100 km are reported for this transverse fault and tonalite and granodiorite intruded along it during the Oligocene [*Mancktelow et al.*, 2001; *Vrabec and Fodor*, 2006]. Together with the SEMP fault and several other minor conjugate faults, the PAL has been active during the extrusion/tectonic escape process. Despite its obvious importance for younger Alpine tectonics, it neither shows noticeable seismic activity nor has it been identified clearly by the TRANSALP seismic reflection data [*Lüschen et al.*, 2004].

[12] The Southern Alps are characterized by a south-vergent fold and thrust belt, which formed in the Miocene as a late stage of the Alpine collision. Along Alp01, a Mesozoic carbonate nappe (Julian Alps) lies on top of Paleozoic schists and clastic rocks. The External Dinarides join the Southern Alps at the SAT [*Doglioni and Bosselini*, 1987]. A supposed detachment plane for the thrusts in the External Dinarides is located at the top of Paleozoic clastic rocks [*Placer*, 1999a]. The depth to Paleozoic rocks is highly variable, reaching more than 10 km. A series of W-E to NW-SE trending dextral faults cuts the Southern Alps [*Placer*, 1996] and the External Dinarides [*Poljak et al.*, 2000; *Zupančič et al.*, 2001] with Cenozoic displacements of up to 70 km (Southern Alps) and 120 km (External Dinarides). Most of these faults have evidence of historical or recent seismicity.

[13] Continued post-early Miocene underthrusting of the Adriatic foreland and External Dinarides formed steep, NW-SE striking reverse faults (for example, Cicarija thrust) and an imbricate belt extending from the northeastern rim of Istria southward to the costal islands [*Vrabec and Fodor*, 2006]. The less deformed southern part of the Adriatic microplate is exposed mainly in the Istria Peninsula [*Poljak et al.*, 2000], which is a carbonate platform that is over 5 km thick. A series of flysch basins is encountered between the South Alpine thrust and the southern end of the Istria Peninsula (Figure 2b).

### 4.2. Tectonic Setting of the Alp02 Profile

[14] The western part of the Alp02 profile (Figures 2a and 2c) obliquely crosses the Tauern window and the Austro-Alpine nappe system. The central part of Alp02 is sub parallel to the PAL, crossing it at km 220. Highly deformed rocks in a WNW-ESE trending metamorphic belt are related to this part of the PAL in Austria and Slovenia [*Fodor et al.*, 1998]. Further to the east, the Alp02 profile enters the Southern Alps, extending south of the dextral transverse and transpressive structures related to the PAL [*Poljak*, 2000; *Placer*, 1999b; *Vrabec and Fodor*, 2006]. Folding and uplift in this transpressive region started at the end of the Miocene [*Tomljenović and Csontos*, 2001]. After crossing the SAT, the Alp02 profile enters the Internal Dinarides. Triassic carbonates and Cretaceous units (mostly plutonic and volcanic) crop out between areas covered by Neogene sediments. Following the course of Alp02, the Internal Dinarides are covered by the sediments of the Sava depression. This depression belongs to the Pannonian basin and has been well explored by seismic reflection profiles as part of oil exploration efforts [*Saftić et al.*, 2003]. The maximum depth of the Neogene sediments is about 5 km.

[15] The Pannonian basin, formed during roll back of the Carpathian subduction represents an unconstrained margin to the Alpine orogen in the east. Lateral extrusion or tectonic escape to this unconstrained margin has been active since the Late Oligocene and begins to the west in the Tauern window and forms dominant structures further east. Several conjugate NW-SE and NE-SW oriented strike-slip faults (for example, PAL and SEMP) and N-S oriented normal faults (not shown in Figure 2a) determine the kinematics of escape and upper crustal thinning. *Linzer et al.* [2002] found that N-S compression since Early Miocene has been compensated by a minimum of 120 km of east-west extension. Eastward displacement of the crust, measured by GPS [*Grenerczy and Kenyeres*, 2006], and seismic activity of several strike-slip faults [*Reinecker and Lenhardt*, 1999] show that tectonic escape of parts of the Alpine orogen toward the Pannonian Basin is an ongoing process.

[16] The Mid-Hungarian zone (MHZ) separates the Alcapa and Tisza units of the Pannonian basin [*Tomljenović and Csontos*, 2001]. It has been a zone of repeated tectonic inversions [*Csontos and Nagymarosy*, 1998] since Eocene times. Periods of thrust faulting were followed by phases of extension and transtension. At the southeastern end of Alp02, the Tisza unit forms the northeast hinterland of the Internal Dinarides (Figure 2) and consists of Mesozoic cover on Paleozoic and Proterozoic basement with a mostly high-grade Variscan metamorphic imprint [*Pamić et al.*, 2002a, 2002b]. Neogene deposits of the Sava depression cover most of the Tisza unit.

## 5. Seismic Wave Field

[17] The *P* wavefield on Alp01 and Alp02 record sections has a high signal-to-noise ratio in the northern (Bohemian massif) and southeastern (Sava depression) parts of the profile. In the Alpine part of the investigation area, data quality is variable, and phase correlations are sometimes not as clear as to the north or southeast. Identification and correlation of seismic phases was done manually on a computer screen using software that allows for scaling, filtering, and varying the reduction velocity [*Zelt*, 1994; *Środa*, 1999]. Examples of record sections for both profiles are shown in Figures 3–5, and synthetic seismograms and ray diagrams calculated for the final velocity models are shown in Figures 6–8 for Alp01 and in Figures 9 and 10 for Alp02.

[18] Clear arrivals of refracted and reflected waves from the crystalline crust and the upper mantle are typically observed up to offsets of 200–250 km and for some shots even to over 350 km (for example, SP31100, Figure 7a). Waves traveling in the sedimentary cover (Psed) of the Pannonian or Molasse basins are observed as first arrivals in the vicinity of a few shotpoints up to offsets of about 10 km (for example, SP32070, Figure 10a). The direct wave in the crystalline crust (Pg) is recorded in some areas at offsets of up to 100–180 km with an apparent velocity in the range 5.6–6.4 km/s. Amplitudes of midcrustal reflections (Pc) are strong for some parts of the profiles, while for other parts they are weak. However, they are usually well correlated (for example, Figure 3b). Reflections from the Moho (PmP) are observed either as a strong, short pulse or with a 1- to 2-s-long coda. There are also some areas, where PmP is weak or not observed at all. The Moho refractions (Pn) are strong on only a few record sections (for example, Figures 5b and 5c). Usually they are weaker but can still be correlated over several tens of kilometers (for example, Figure 3). For some shotpoints (for example, Figures 3c and 5c), well-developed overcritical crustal phases (Pcrustal) can be correlated by their envelopes.

[19] Examples of seismic wavefields in the area of the Bohemian massif and the Molasse basin are shown in Figures 3 and 6a. These areas are characterized by strong Pg phases with apparent velocities of 5.6–6.1 km/s. Especially for the Bohemian massif, Pcrustal phases are observed up to

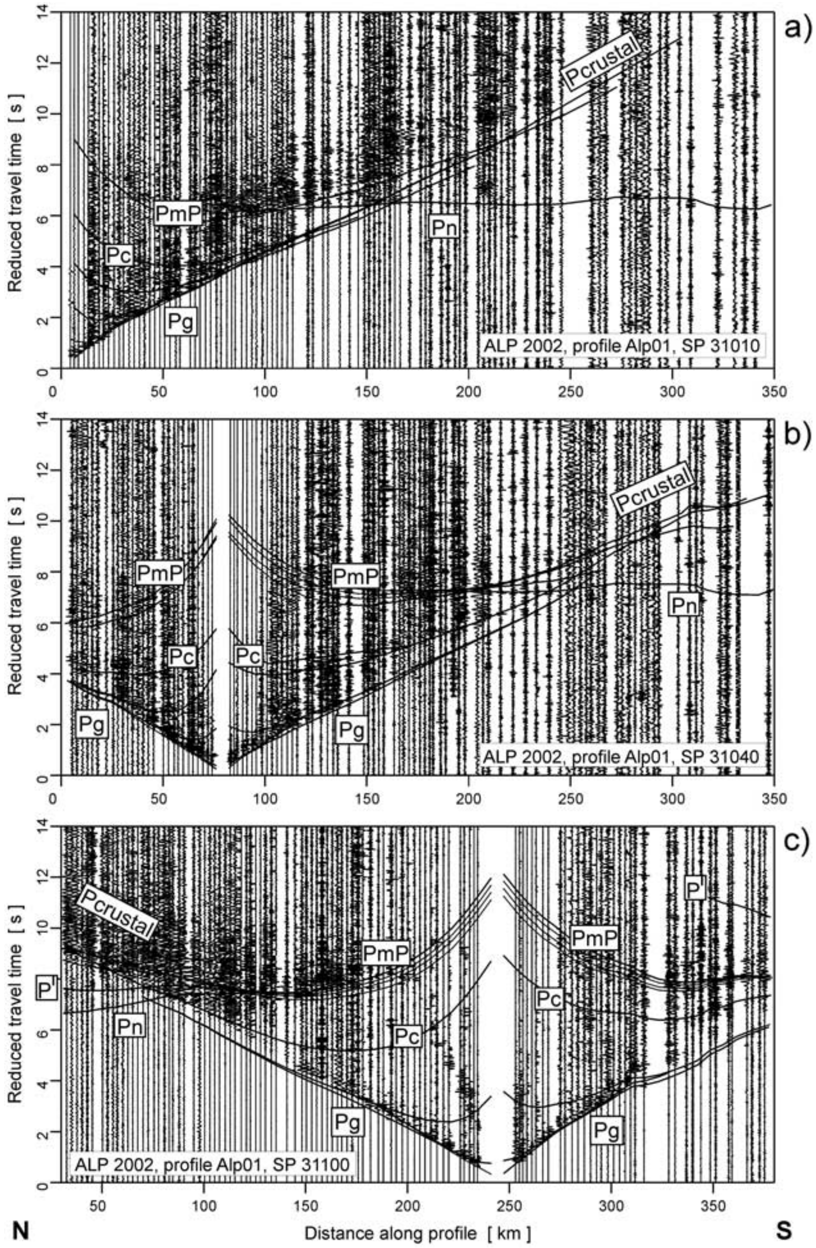


**Figure 3.** Alp01, interpretation of seismic wavefields (traces are normalized, reduction velocity is 8 km/s); correlation of Pg, Pn, PmP, and undercritical and overcritical crustal phases (Pc, Pcrustal): (a) SP31010, (b) SP31040, (c) SP31100. The multiple PmP in Figure 3b and Figure 3c represents a crust-mantle transition (see text).

about 250-km offsets with a relatively low apparent velocity of about 6.4 km/s (for example, SP 31010 in Figure 3a). Pg phases diving to the middle and lower crust are correlated as secondary arrivals at long offsets where they merge with Pc and Pcrustal.

[20] As expected, the wavefield observed in the Eastern and Southern Alps is more complex (Figures 3c, 4a, 5a, 5b, 7a, 9a, and 10a). Strong first arrivals (Pg) are distinct up to 60- to 90-km offsets and are characterized by large variations in apparent velocity and amplitude. The contact between the Molasse basin and the Eastern Alps is visible along Alp01 (at a distance of about 300 km) as a barrier for the propagation of Pg waves (Figure 4a). Midcrustal reflections (Pc) are usually recorded at short distance intervals (20–50 km) and are characterized by variations in apparent velocity, amplitude, and coda. They are much weaker than midcrustal reflections recorded in the Bohemian massif. On the other hand, Moho reflections are usually strong, well-correlated short pulses (Figure 8a). Pn arrivals are only fragmentarily recorded in the Eastern Alps. Also, Pcrustal waves are not observed for shots in the Eastern Alps.

[21] In the area of External Dinarides and the Adriatic foreland, the Pg phase has very high velocity (see Figures 4b and 4c, where the velocity at reciprocal traveltimes between SP31150 and SP31160 is about 6.4 km/s). Relatively small amplitudes characterize waves from the middle

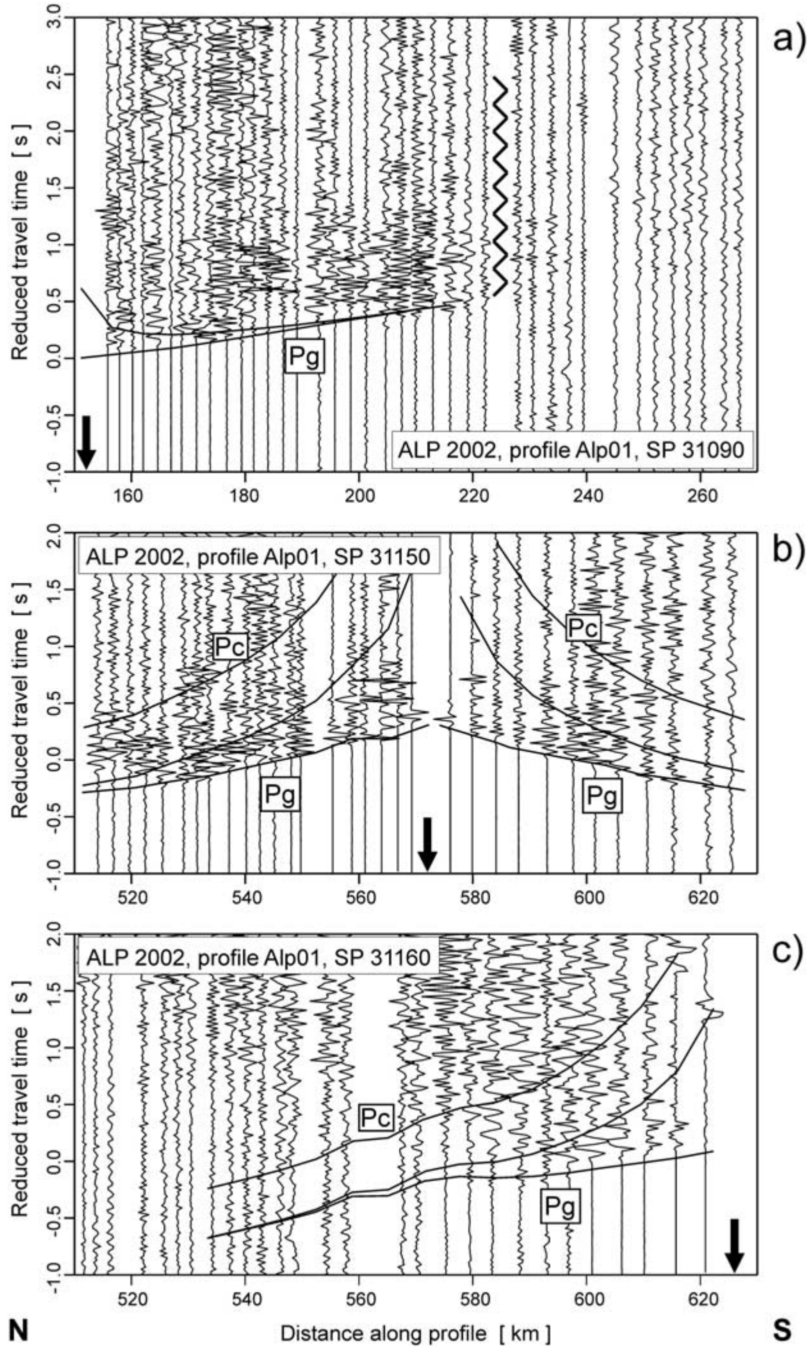


**Figure 4.** Alp01, interpretation of seismic wavefields (traces are normalized, reduction velocity is 6 km/s, arrows mark shot locations): (a) SP31090, correlation of Pg; observe damping of Pg beyond profile distance 220 km (wiggly line, Molasse basin), (b) SP31150 and (c) SP31160, correlation of Pg and Pc; note high Pg velocities (about 6.4 km/s) in the External Dinarides and the Adriatic foreland.

crust, which indicates small contrasts at seismic boundaries and small velocity gradients within layers. A variation in PmP-phase arrival times of >2 s at critical distances indicates a large variation in the Moho depth at the southern termination of Alp01 (Figures 8a and 8b).

[22] The southeastern part of the profile Alp02 extends from the Internal Dinarides into the Pannonian basin. Examples of records from this area are shown in Figures 5b, 5c, and 10a. Thick sediments of the Sava depression cause significant undulations of Pg traveltimes (for example, Figure 10a to the east). The variation of PmP traveltimes that is particularly visible for SP32050 (Figure 9a) indicates thick Alpine and thin Pannonian crust. For both shotpoints in this area (SP32070, SP32080), a clear Pn phase is observed over an offset range of 120 km to over 200 km (Figures 10 and 5c).

[23] Well-correlated waves ($P^{\mathrm{I}}$) from the mantle lithosphere were modeled as reflections and were observed from

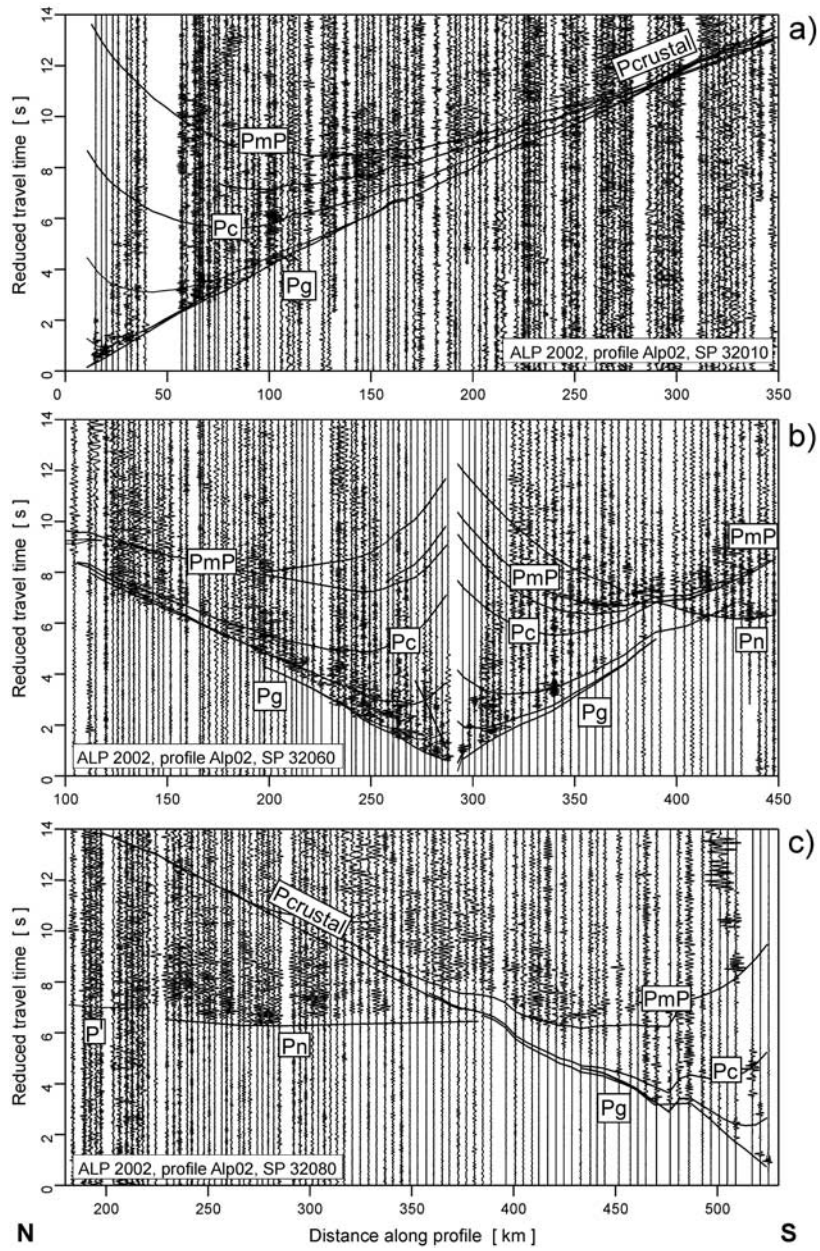


**Figure 5.** Alp02, interpretation of seismic wavefields (traces are normalized, reduction velocity is 8 km/s): (a) SP32010, correlation of Pg, Pn, PmP, and undercritical and overcritical crustal phases (Pc, Pcrustal). (b) SP32060, correlation of Pg, Pn, PmP, and Pc; see more complicated wavefield to *S* comparing to *N*. (c) SP32080, correlation of Pg, Pn, PmP, and undercritical and overcritical crustal phases (Pc, Pcrustal); note amplitude reduction of Pn from profile distance 230–220 km ($P^{I}$); for explanation, see text.

shotpoints in the central part of Alp01 recorded toward the south at offsets of 250–350 km (Figure 7a).

## 6. Derivation of Crustal Models

[24] In the Molasse basin and the Sava depression (Figures 2b and 2c), information on basin depth and *P* wave velocity is available from exploration seismology [*Brix and Schultz*, 1993; *Saftić et al.*, 2003]. This information provides more detailed models of the uppermost structure (down to 3- to 7-km depth) than can be obtained from the ALP 2002 data alone. The lateral extent of the NCA and TW was determined from a geological map (Figure 2a), and their velocities were taken from the TRANSALP tomographic model after the work of *Bleibinhaus and Gebrande* [2006]. Initial models of the deeper structure and the Moho were generated by tomographic inversions of first arrivals using the method of *Hole* [1992]. The inversions were carried out using three-dimensional corridors covering all shots and receivers. The size of the grid cells was 1 × 1 × 1 km. A total of 729 first arrivals (Pg and Pn phases) were picked for Alp01, and 433 were picked for Alp02

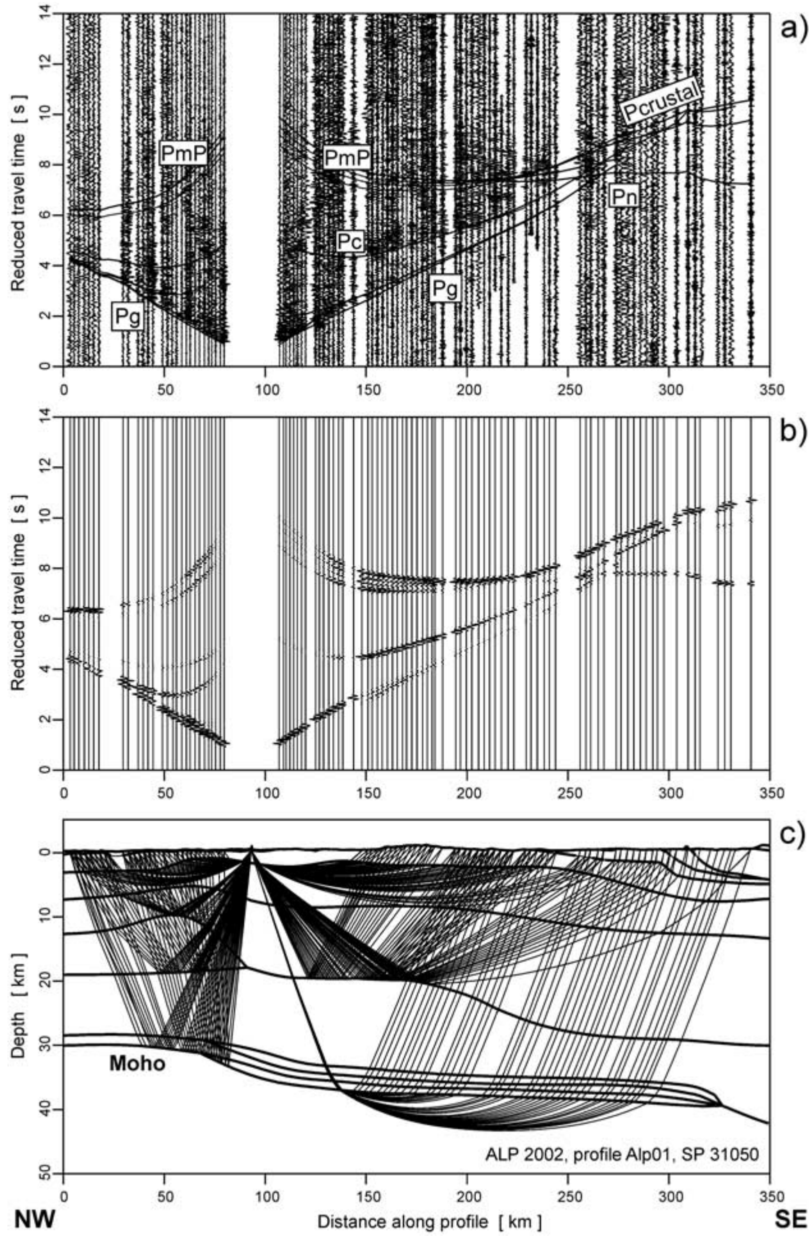


**Figure 6.** Alp01, interpretation and modeling of record section for SP31050: (a) Seismic wavefield (traces are normalized, reduction velocity is 8 km/s), correlation of Pg, Pn, PmP, and undercritical and overcritical crustal phases (Pc, Pcrustal). (b) Synthetic seismogram; note correctly modeled strong midcrustal phase Pc. (c) Raypath diagram with chosen rays; for explanation of layered Moho, see text.

(Figures 11a and 12a). The penetration depth of the inversion was increased stepwise by successively selecting larger maximum offsets. The results of these inversions are shown in Figures 11c and 12c. The three-dimensional velocity models were averaged along the corridor axis normal to the profiles in order to generate two-dimensional profiles. The standard deviations of traveltime residuals are ±0.07 s for Pg and ±0.24 s for Pn phases (Figures 11b and 12b). The Molasse basin and Sava depression are clearly visible in the tomographic models. Pg ray coverage is sparse, and initial models for crustal velocities were generated by extensive smoothing (see velocity contours in Figures 11c and 12c). Pn ray coverage is even smaller, and continuous values of the Moho depth were extracted from the Moho map of *Dèzes and Ziegler* [2001]. The ray coverage is shown in Figures 11c and 12c together with the diving wave tomographic inversion results.

[25] The tomographic inversion results, and other above mentioned a priori data were used to create starting models for detailed two-dimensional forward modeling of refracted and reflected phases (precritical and postcritical) that was undertaken using the following ray-tracing techniques. The calculations of traveltimes, rays, and synthetic seismograms were made using the ray-theory package SEIS83 [*Červeny and Pšenčík*, 1983] enhanced by employing the interactive graphical interfaces MODEL [*Komminaho*, 1997] and

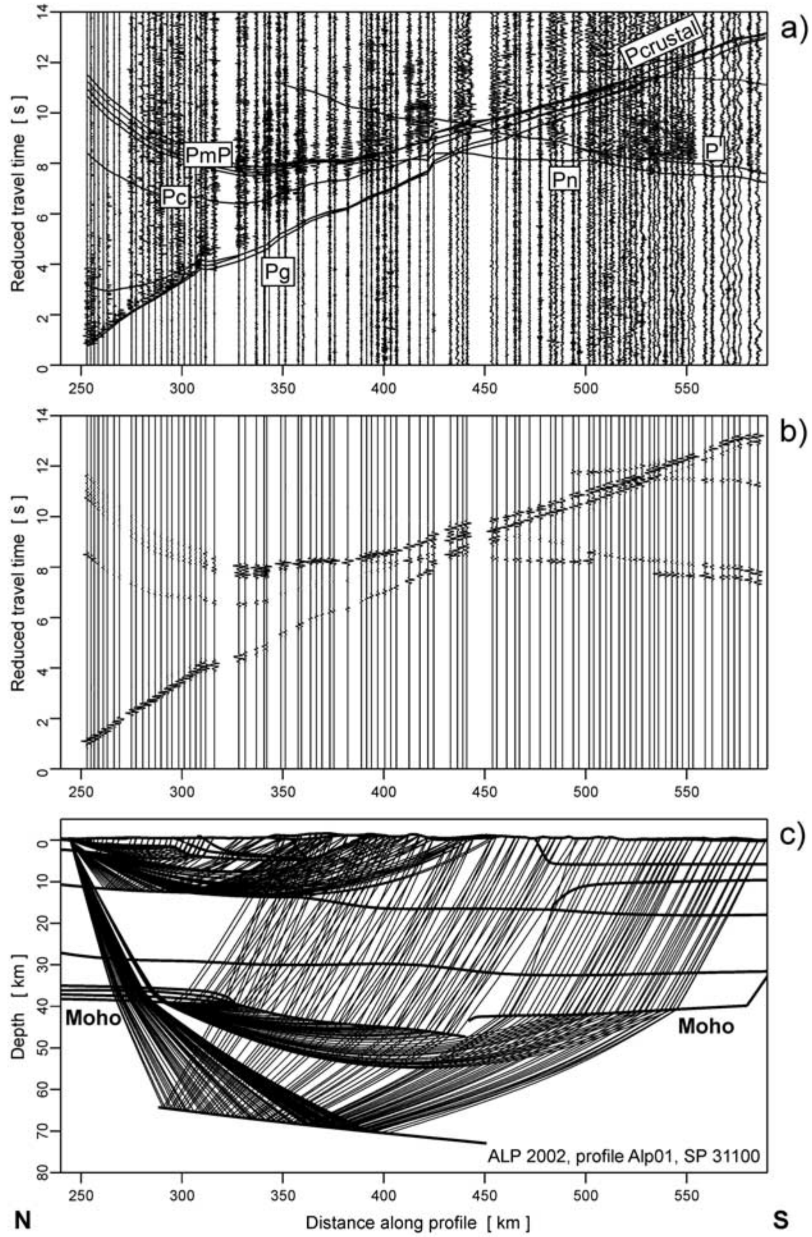


**Figure 7.** Alp01, interpretation and modeling of record section for SP31100: (a) Seismic wavefield (traces are normalized, reduction velocity is 8 km/s), correlation of Pg, Pn, PmP, undercritical and overcritical crustal phases (Pc, Pcrustal), and upper mantle reflection ($P^{\mathrm{I}}$). (b) Synthetic record section. (c) Raypath diagram with chosen rays, particularly Pn and reflection from mantle lithosphere ($P^{\mathrm{I}}$).

ZPLOT [*Zelt*, 1994] with modifications by *Środa* [1999]. The velocity model was successively altered by trial and error, and traveltimes were recalculated many times until agreement was obtained between observed and model-derived traveltimes. In addition to traveltime modeling, synthetic seismograms were calculated to control velocity gradients within the layers and the velocity contrast at the seismic boundaries. The SEIS83 package calculates reflection coefficients considering converted waves. The Vp/Vs ratio was chosen between 1.73 and 1.80, the density ($d$) was derived from the relation $d = (1700 + 0.2\ \mathrm{Vp\ m^{-1}\ s})\ \mathrm{kg\ m^{-3}}$ according to SEIS83 [*Červeny and Pšenčík*, 1983]. The final synthetic seismograms show good qualitative agreement with the relative amplitudes of observed refracted and reflected waves.

[26] The final velocity models along profiles Alp01 and Alp02 are presented in Figures 13 and 14, respectively, and show large lateral variations in the structure and thickness of the crust. Along the Alp01 profile, a significant structure (reflector) in the upper mantle was also modeled.

### 6.1. Velocity Model for the Alp01 Profile

[27] To the north (profile distance 0–230 km), Alp01 crosses the Bohemian massif (Saxothuringian, Barrandian, and Moldanubian units, Figure 2). In this part of the profile, crystalline rocks are exposed at the surface or with only thin

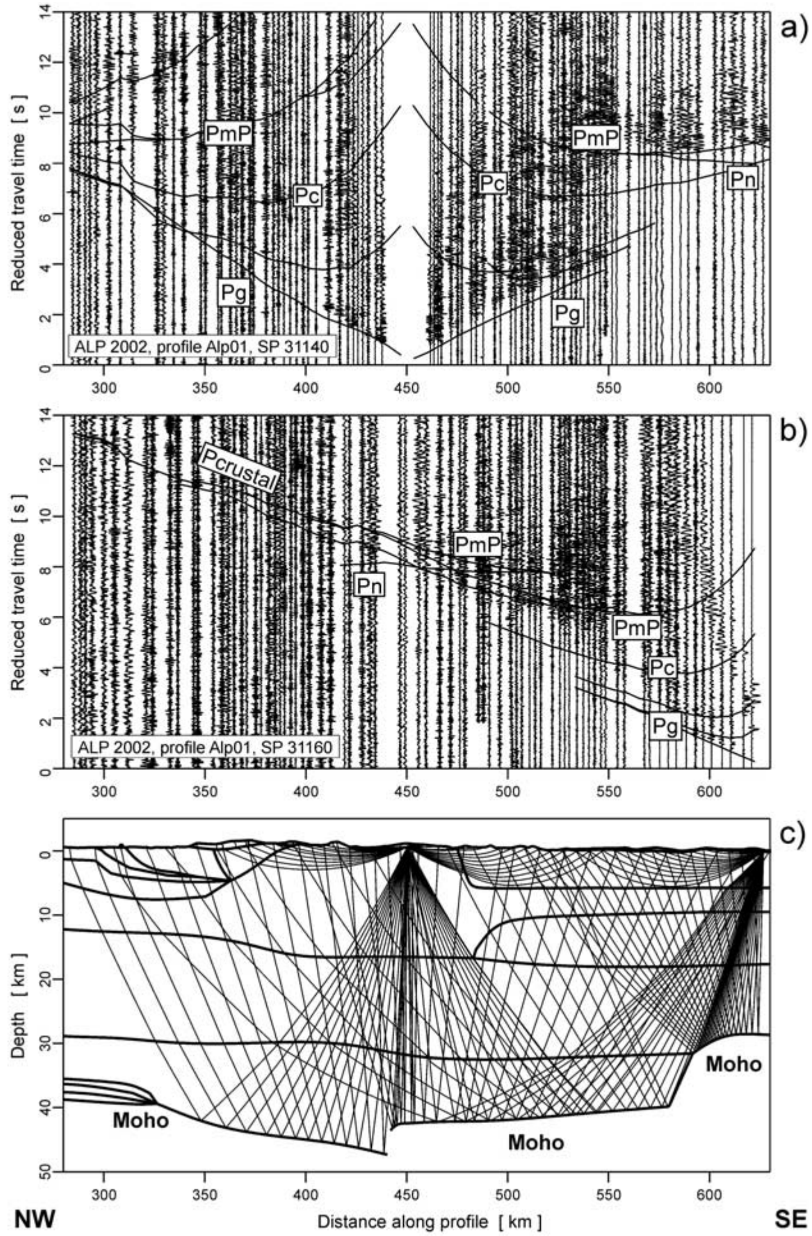


**Figure 8.** Alp01, seismic data supporting Moho jump at profile distance 580 km: (a) SP31140, Seismic wavefield (traces are normalized, reduction velocity is 8 km/s), correlation of Pg, Pn, PmP, and Pc. (b) SP31160, seismic wavefield (traces are normalized, reduction velocity is 8 km/s), correlation of Pg, Pn, PmP, and undercritical and overcritical crustal phases (Pc, Pcrustal). (c) Raypath diagram for SP31140 and SP31160 with chosen rays. Observe ~2-s time difference of PmP phase reflected at Moho boundary north of Moho jump (record section SP31140) and south of it (SP31160).

sedimentary cover, and basement velocities of 5.6–5.8 km/s were found at less than 1-km depth (Figure 13). In the Molasse basin, low-velocity (2.5–4.5 km/s) sediments extend down to about 5-km depth. High-velocity gradients in the uppermost crust followed by low gradients in the middle crust are a characteristic feature of most of the Bohemian massif. However, in the middle crust (10–19 km) of the Saxothuringian unit (distance interval ~20–80 km), a body with relatively high velocity was delineated (Vp ~ 6.5–6.6 km/s). Under the Molasse basin, the velocity structure of the crystalline crust is similar to that of the adjacent Bohemian massif. Thus, the crust of both the southern Bohemian massif and Molasse basin is characterized by relatively low velocities 6.0–6.5 km/s down to the Moho (30–38 km). These low velocities are well documented by overcritical crustal arrivals Pcrustal at offsets of 150–280 km (for example, Figure 3a) and generally agree with the velocity model for the CEL09 profile [*Hrubcová et al.*, 2005] in the vicinity of where it crosses Alp01. Beneath the Bohemian massif and the Molasse basin, strong mid-crustal reflections from a depth of 20–30 km (see Pc phase in Figure 3) must have been generated by a large impedance

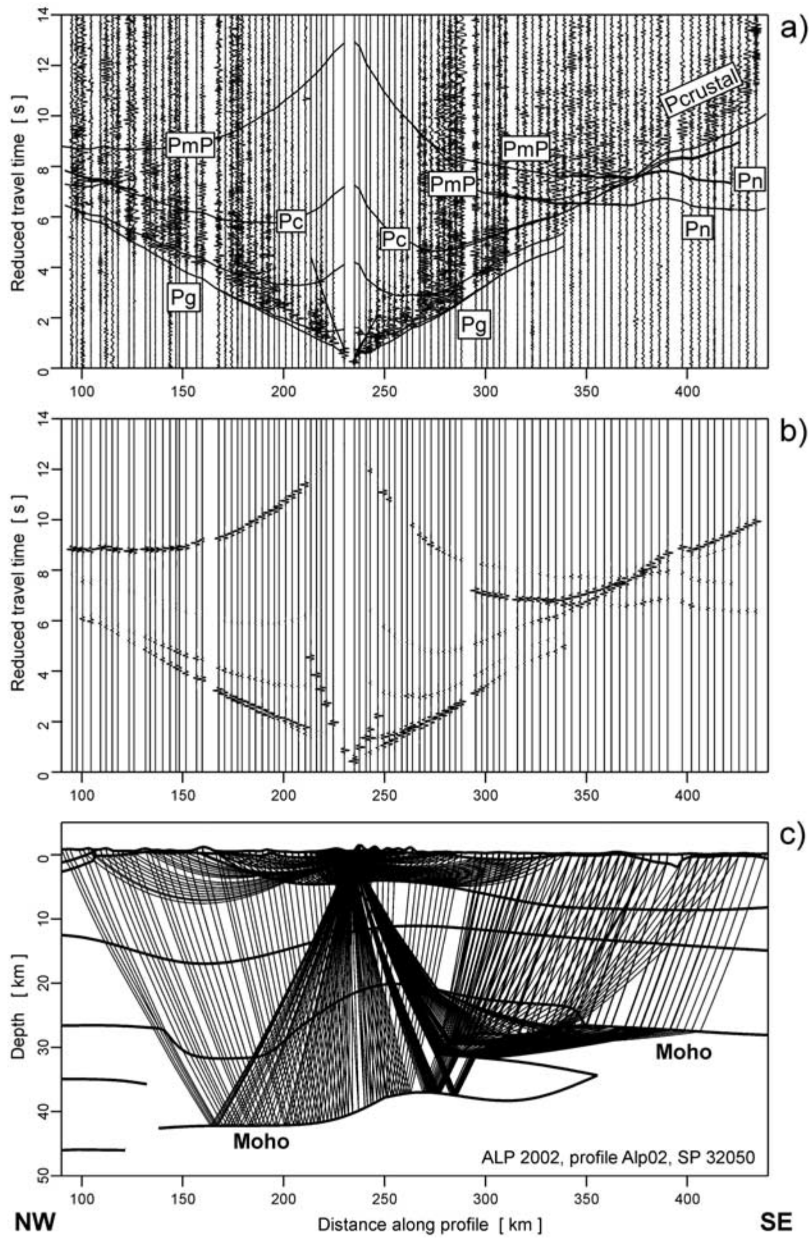


**Figure 9.** Alp02, interpretation and modeling of record section for SP32050: (a) seismic wavefield (traces are normalized, reduction velocity is 8 km/s), correlation of Pg, Pn, PmP, and undercritical and overcritical crustal phases (Pc, Pcrustal); note two PmP and Pn phases in SE direction. (b) Synthetic record section. (c) Raypath diagram with chosen rays.

contrast near the boundary between the middle and lower crust. However, a large velocity contrast between thick layers is inconsistent with the low velocities observed from Pcrustal waves. To model the amplitudes of the Pc waves, we used thin (<1 km) high-velocity 'floating reflectors' with a velocity contrast of about 0.4 km/s (compare synthetic and observed Pc waves in Figure 6a and 6b). However, the physical nature of the 'floating reflectors' is not clear because their polarity cannot be detected unequivocally. On the other hand, the observed amplitudes of PmP waves generated beneath the Bohemian massif and the Molasse basin are similar in amplitude to those from the beneath the Alpine part of the profile, where velocities in the lower crust are higher. Using large velocity contrasts in the transition from the low-velocity lower crust to the uppermost mantle (velocities 6.4–6–5 km/s and about 8.1 km/s, respectively) produced amplitudes that were too large in the synthetic seismograms. To solve this problem, we found that a high-velocity gradient and/or a laminated transition zone with a thickness of a few kilometers in the lowermost crust (Figure 13) produced a fit to the observed amplitudes. This thin 'layer' did not produce overcritical phases in the synthetic seismograms (which in fact are not observed) and reduces PmP phase amplitudes.

[28] The most complicated crustal structure is observed beneath the Molasse basin and between the NAT and the TW (distance interval 250–430 km, Figure 13). This is an

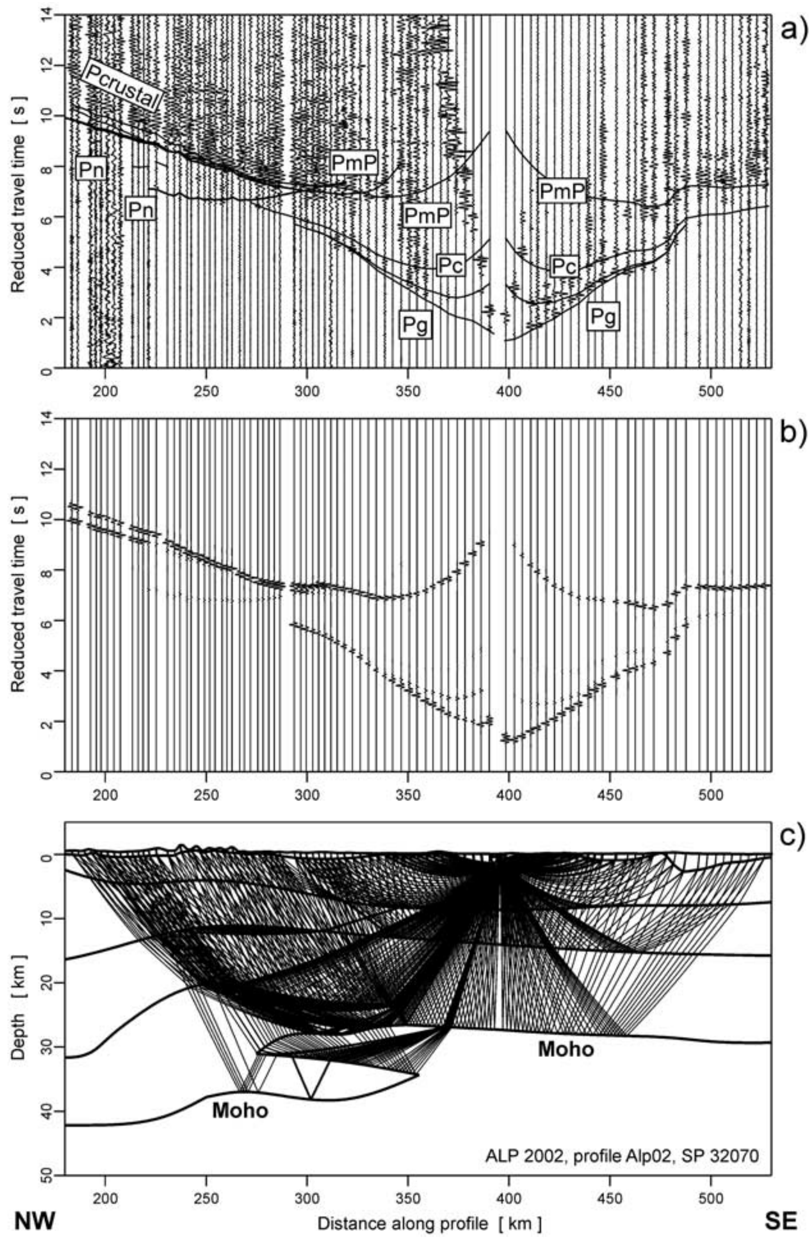


**Figure 10.** Alp02, interpretation and modeling of record section for SP32070: (a) seismic wavefield (traces are normalized, reduction velocity is 8 km/s), correlation of Pg, Pn, PmP, and undercritical and overcritical crustal phases (Pc, Pcrustal); note influence of sedimentary basin for Pg and PmP waves in SE part of profile and two modeled PmP and Pn phases in NW direction. (b) Synthetic seismogram. (c) Raypath diagram with chosen rays.

area of pronounced topography (shot/receiver elevations vary from 500 to 1700 m) and complex structure in the accretionary wedge. From the NCA (northern boundary of Eastern Alps) to the PAL (southern boundary of Eastern Alps), the Moho deepens from ~38 to ~47 km (see also Figure 7). Under the PAL, at ~440 km along the profile, the Moho steps up to a shallower level. This Moho depth is again well resolved by PmP and Pn arrivals, decreasing slightly from 42 to 40 km toward the south. A midcrustal reflector south of PAL at ~32 km depth is not as pronounced as in the northern part of the profile, but it is also well documented by Pc arrivals (Figures 3c and 8a). In the distance range of 460–480 km, a 'floating reflector' also explains large amplitude Pc arrivals.

[29] The PAL (profile distance 450 km), as the boundary between the Eastern and the Southern Alps, does not correlate with any intracrustal structure revealed by our model. Under the Southern Alps, the structure of the upper crust changes significantly. Further to the south, the External Dinarides and the Adriatic foreland are characterized by a high-velocity basement, with velocities of about 6.2 km/s close to the surface and about 6.4 km/s at 6-km depth. Below this depth, a low-velocity zone (LVZ) with velocities <6.2 km/s extends down to 25 km. At the southern end of

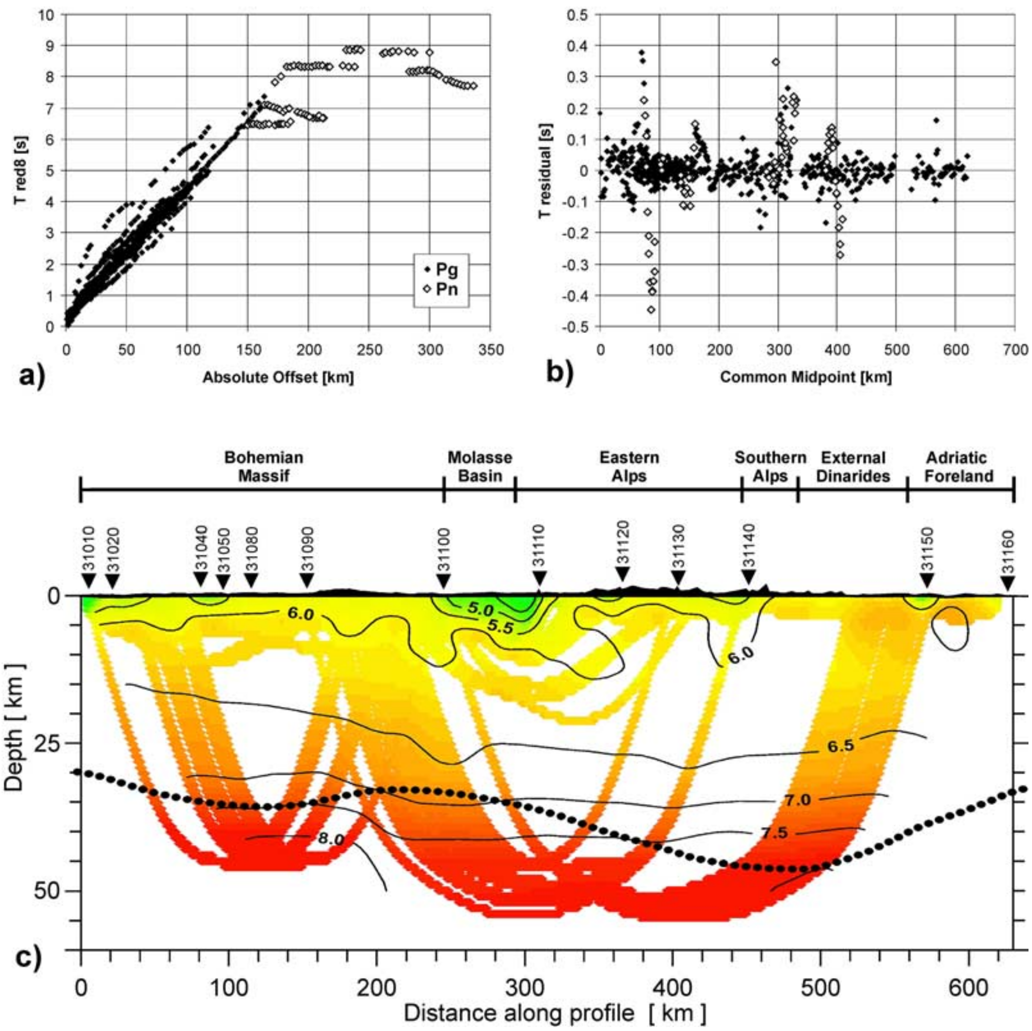


**Figure 11.** Alp01 profile, two-dimensional tomographic inversion of first arrival traveltimes. (a) Traveltime picks for first arrival traveltimes (Pg dots, Pn circles). (b) Traveltime residuals for the final model. (c) *P* wave velocity model for given ray coverage; interpolated velocity contours; Moho depth (dotted black line) according to Moho map of *Dézes and Ziegler* [2001] is superimposed.

the profile, a pronounced shallowing of the Moho from 40 to 28 km was found. A comparison of the PmP phases in the record sections of SP31140 (Figure 8a) and SP31160 (Figure 8b) and the corresponding ray diagrams (Figure 8c) document these different levels of the Moho. The ray diagram also shows that Pn cannot be observed from the shallow Moho because this feature is at the edge of the model.

[30] The velocity in the uppermost mantle determined from Pn traveltimes is 8.10–8.20 km/s below the Bohemian massif, the Molasse basin, the Eastern Alps and Southern Alps, and the External Dinarides. The velocity in the shallow mantle of the Adriatic foreland (8.08 km/s) follows only from amplitude modeling of PmP and should not be compared with the other values. The reflector in the lower lithosphere is well resolved between profile distances of 300–440 km. It lies ~25 km below the Moho and parallels the southward dipping Moho in this part of the profile (Figure 7).

### 6.2. Velocity Model for the Alp02 Profile

[31] The crustal structure along the Alp02 profile (Figure 14) indicates that two domains are present, the Eastern Alps to the west and the Pannonian basin represented by the Sava depression (Internal Dinarides and Tisza unit) to the east. These two blocks are separated by a transition zone below the Southern Alps in the distance range of 220–340 km.

[32] The sedimentary layers in the narrow valleys and small basins of the Eastern Alps are not significant at the scale of our investigation and are only partly resolved by our measurements. The individual basins of the Sava depression along Alp02 are 1–3 km deep according to the data from hydrocarbon exploration efforts [*Saftić et al.*, 2003]. The uppermost basement along the whole profile is characterized by velocities of about 5.7–5.9 km/s, with the exception of a west-dipping thin slab between 80- and 110-km profile distance. This slab has a high velocity (about 6.6 km/s) and extends down to about 3-km depth. Although the thickness of this slab is somewhat ambiguous, its high velocity and western dip are well constrained by reversed

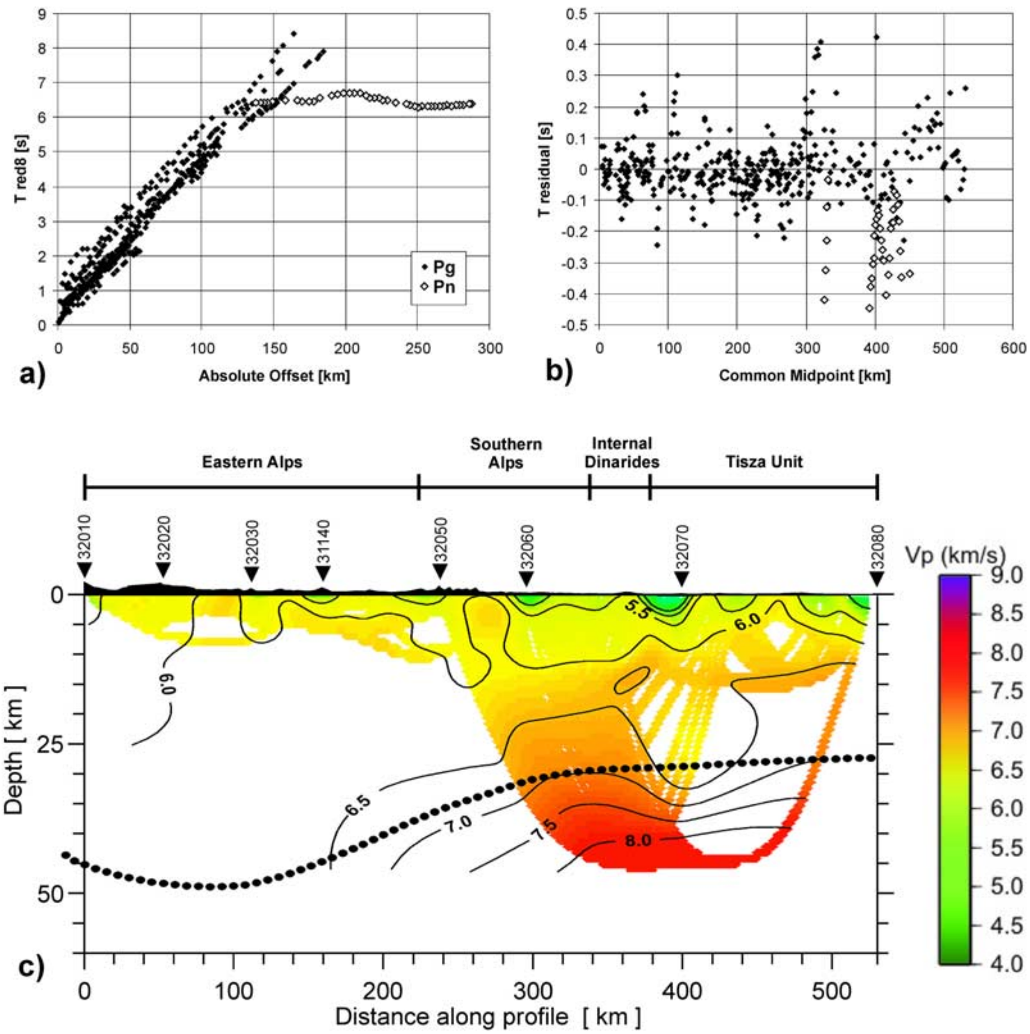


**Figure 12.** Alp02 profile, two-dimensional tomographic inversion of first arrival traveltimes. (a) Traveltime picks for first arrival traveltimes (Pg dots, Pn circles). (b) Traveltime residuals for the final model. (c) *P* wave velocity cross section for given ray coverage; interpolated velocity contours; Moho depth (dotted black line) according to Moho map of *Dézes and Ziegler* [2001] is superimposed.

first-arrival observations from the neighboring two shot-points. All across the model in the depth range of 10–30 km, velocities range from 5.8 to 6.5 km/s. The lowest velocities occur between 300 and 400 km along the profile (mainly in the area of the Internal Dinarides). In the Eastern Alps, similar to profile Alp01, a strong reflection from a depth of about 26 km was modeled as a 'floating reflector' with a velocity contrast of 0.35–0.4 km/s. Another reflector with a velocity contrast of 0.3 km/s was found at 35-km depth in the distance interval 50–130 km. Lower crustal velocities in the Eastern Alps range from 6.45–6.85 km/s, slightly higher than beneath the Alp01 profile. Midcrustal interfaces and velocities were constrained to match Alp01 at the intersection.

[33] From the west end of Alp02 to a distance of about 120 km, no Pn phases could be identified. Only fragmentary PmP phases suggest that the Moho is at a depth of ~46 km (Figure 5a). Further to the east (~130 km), the Moho rises to a depth of 43 km and rises again to ~37 km at a distance of ~250 km. Southeastward of this point, which lies beneath the Southern Alps, the modeled structure becomes complex. The Moho depth decreases abruptly to 27–29 km in the region that coincides with a pronounced transition from the high surface elevation of the Alpine domain to the low elevations of the Pannonian domain, which comprises the easternmost portion of the Southern Alps, the Pannonian basin including the Sava depression, and the outcrops of the Internal Dinarides and the Tisza Unit. The shallow Moho persists to the east end of Alp02 and is well constraint by PmP and also some Pn onsets from shots SP32050, 32060, 32070, and 32080 (Figures 9, 5b, 10, and 5c). The uppermost mantle velocities are 8.05 km/s for the Southern Alps and Internal Dinarides and 7.95 km/s for the Sava depression. Below the Eastern Alps, uppermost mantle velocities are not constraint by Pn traveltimes. In the Pannonian domain, the amplitudes of Pn are strong. A steeply dipping or vertical step of the Moho at the profile distance 280-km models observed traveltimes well. However, in order to model the fading amplitudes of this phase to the west, a "crocodile-like" structure with a velocity inversion was introduced (Figures 9c and 10c). Therefore a double Moho

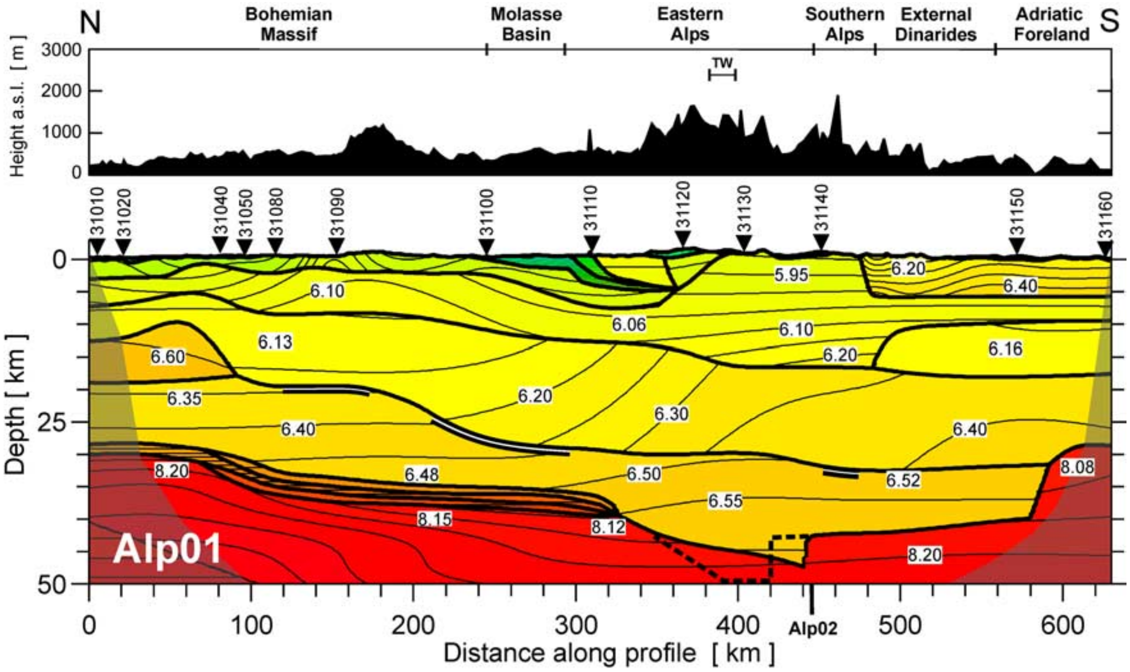


**Figure 13.** Alp01, *P* wave velocity model (4:1 vertical exaggeration) derived from forward modeling by ray tracing with elevation (25-fold vertical exaggeration) on top; for velocity color bar, see Figure 14; thin lines are isovelocity contours in kilometers per second, medium thick solid lines are layer boundaries, double solid lines represent "floating reflectors" and thick dashed line represents steeply dipping Moho boundary below the Tauern window (for explanation see text); grey portions of the model have no ray coverage; numbered triangles refer to shotpoints; intersection with profile Alp02 is at profile distance 448 km.

may exist according to our interpretation over a distance of >30 km at the transition between the Alpine and Pannonian domains.

## 7. Analysis of Accuracy, Resolution, and Uncertainties

[34] In our modeling, calculated traveltimes fit observed traveltimes for both refracted and reflected waves with an accuracy of ±0.1–0.2 s with few exceptions. Picking accuracy for Pg was usually about ±0.05 s and about ±0.1 s for reflected phases (midcrustal reflections, PmP) and Pn phase. Low signal-to-noise ratio and wide geophone spacing may result in larger errors because of uncertainty in phase correlation. In addition, synthetic seismograms generally show good qualitative agreement with the relative amplitudes of observed refracted and reflected waves. Estimates of uncertainty were derived from the range of permissible values for model parameters (velocity, depth) determined during forward modeling and are based on experience obtained earlier from the analysis of POLONAISE'97 and CELEBRATION 2000 profiles [e.g., *Grad et al.*, 2003, 2006]. These efforts were characterized by a similar methodology, source and receiver density, and comparable data quality [*Janik et al.*, 2002; *Grad et al.*, 2003, 2006]. For the upper crust (consolidated basement), where the coverage by Pg waves is the highest, the precision of velocity determinations is ±0.1 km/s. In the uppermost mantle for areas where Pn waves are well recorded, the velocity uncertainty is only a little higher. Although waves refracted from the lower crust are very seldom observed as first arrivals, in many cases, the situation is improved because of well-recorded overcritical crustal waves that penetrate the lower crust, and the precision of the velocity determination here is about ±0.2 km/s. The depths of midcrustal boundaries are usually determined with the accuracy ±2–3 km, and the Moho boundary should have a higher accuracy, ±1–2 km, where the ray coverage is good.

[35] However, in the process of modeling, the limitations of ray theory must be kept in mind. In addition, we must keep in mind that two-dimensional modeling does not take into account out-of-plane refracted and reflected arrivals, which must have occurred particularly in such a structurally complex area as the Alps. Because of these considerations and the lower ray coverage, we have to expect lower accuracy for the Moho depth on Alp01 below the Eastern Alps (profile distance range 360–450 km). An alternative interpretation of Alp01, which achieved also an acceptable data fit, shows the Moho boundary dipping more steeply to a maximum depth of ~50 km below the Tauern window (dashed line in Figure 13 between 340- and 400-km profile distance). Sparse PmP and no Pn data at the western end of Alp02 also result in a poorly constrained Moho depth in this region. The crocodile structure at the Moho step at 270 km along Alp02 is unlikely to be unique in detail. However, we generated a number of alternative models, and all that fit the traveltimes and amplitudes equally well showed a step in

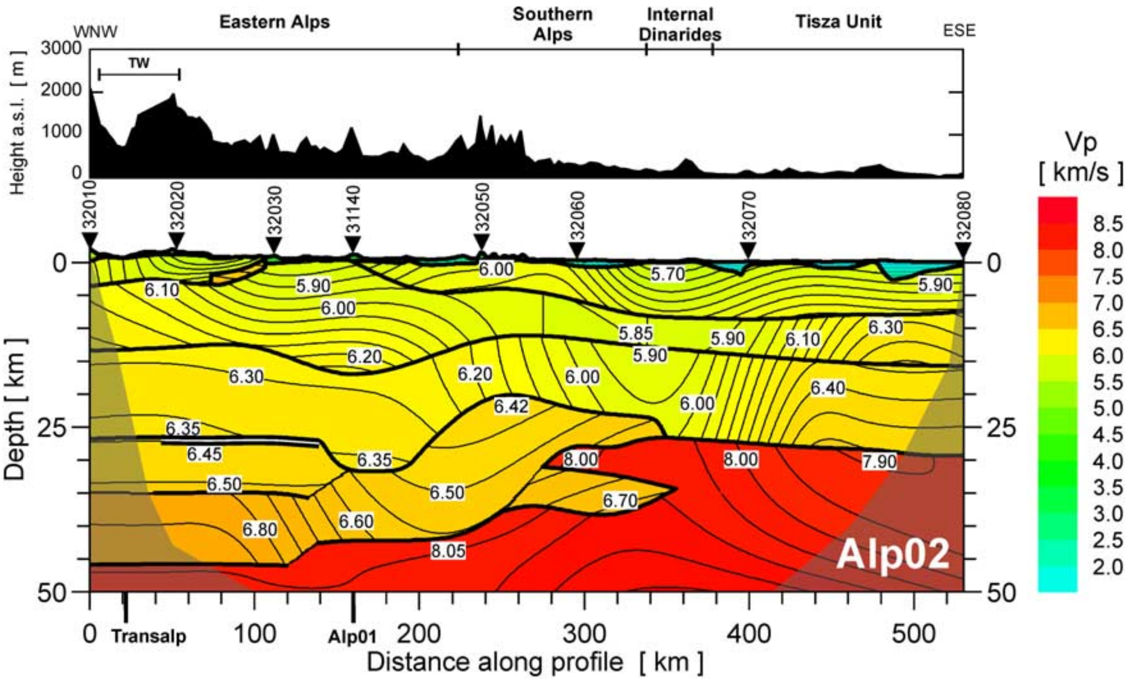


**Figure 14.** Alp02, *P* wave velocity model (4:1 vertical exaggeration) with velocity color bar; for description, see caption of Figure 13; intersection with profile Alp01 is at profile distance 160 km.

Moho depth at the same location and of similar amplitude along with an LVZ beneath the Moho.

[36] In Figure 15, we compare velocity-depth functions for Alp01 and Alp02 with those of prior experiments including CEL09 [*Hrubcová et al.*, 2005], ALP'75 [*Yan and Mechie*, 1989], Lago-Lagorai>Tarvisio>East, SudALP, Eschenlohe>Trieste, ALP'78 (shotpoints *T* to *D''*) [*Scarascia and Cassinis*, 1997], TRANSALP [*Bleibinhaus*, 2003; *Bleibinhaus and Gebrande*, 2006]. Most velocity-depth functions agree in a general way, with velocities varying within a few tenths kilometers per second and layer depths varying within a few kilometers. One significant discrepancy between velocity-depth profiles exists between Alp02 and TRANSALP in the depth range of 4–25 km. The maximum difference of ~0.5 km/s occurs at depth of ~10-km depth, where the Alp02 velocity model is well constrained. The intersection of these profiles is located in the center of the TW and deviations amounting to ~0.5 km/s in the upper and middle crust below the TW are consistent with an anisotropy value of ~10% for the TW with the fast direction oriented E-W as determined by *Bleibinhaus and Gebrande* [2006] and *Bleibinhaus et al.* [2006]. While the TRANSALP model is based on N-S-oriented observations, the Alp02 profile approximately represents the fast E-W direction.

[37] Even though anisotropy may also be significant at other profile intersections, we disregard the influence of anisotropy in the following analysis in order to obtain an estimate of accuracy of *P* wave velocities from the velocity-depth profiles shown in Figure 15. If the accuracy of our interpretations and the older ones are on average equal, the standard deviations of the velocities are ±0.10 and ±0.15 km/s for the *P* wave velocities at depths of 10 and 25 km, respectively. These standard deviations agree with the corresponding uncertainties derived from the analysis of POLONAISE'97 and CELEBRATION 2000 data [e.g., *Janik et al.*, 2002; *Grad et al.*, 2003, 2006].

[38] For comparisons of Moho depth, we have only few intersections where both our new more detailed profiles and the older profiles have sufficient ray coverage. At the intersection of Alp01 and CEL09 in the Bohemian massif, the depth difference is less than 2 km, which is in agreement with our estimated uncertainty. In the Eastern Alps, the ALP'75 profile shows the Moho to be about 5 km deeper than in the Alp01 model. Nearing the vicinity of the PAL at the profile Lago-Lagorai>Tarvisio>East, the Moho is about 3 km shallower than on Alp01 and Alp02. In the following discussion, we will confine our tectonic interpretations only to features that are not sensitive to these uncertainties in the Moho depth.

## 8. Tectonic Interpretation

[39] In the following discussion, we present a tectonic interpretation of the velocity models derived for the Alp01 and Alp02 profiles. Topography of the Moho, Pg velocities, the strength, shape, and continuity of midcrustal reflectors, surface geology, and results from older profiles, especially TRANSALP, ALP'75, and Lago-Lagorai>Tarvisio>East, will be integrated into our interpretation.

### 8.1. Tectonic Interpretation of the Alp01 Velocity Model

[40] The Alp01 profile provides new insights into the structure of the crust and uppermost mantle from the Bohemian massif across the Alps to the Adriatic foreland (Figure 16). At the northern end of the profile, the Moho has a depth of about 28 km, and there is a zone of relatively high velocities in the middle crust (6.60 km/s), which was also emphasized by *Vrána and Štědrá* [1998] in their

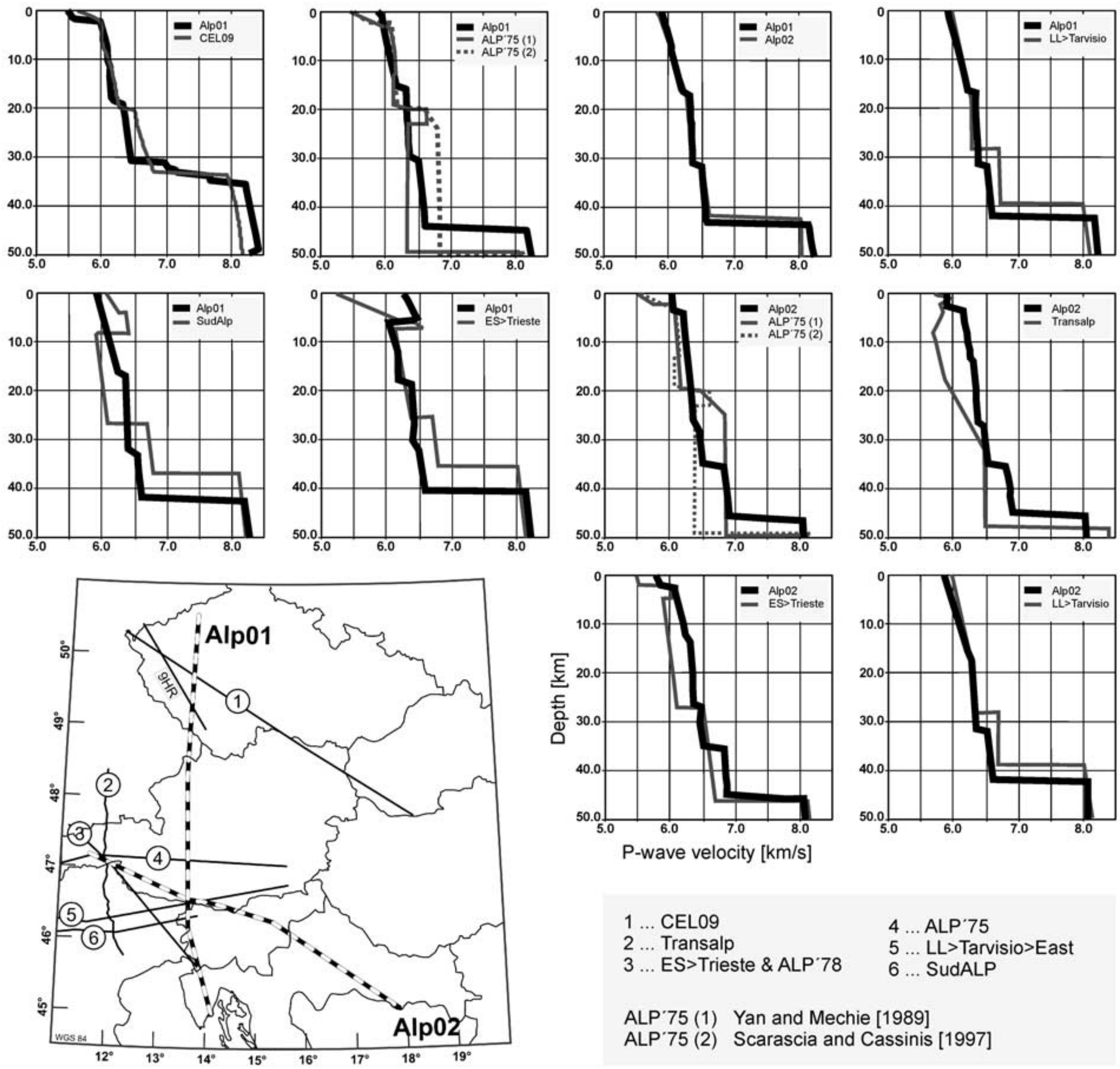


**Figure 15.** Comparisons of velocity-depth diagrams of Alp01 and Alp02 at intersections with older profiles and each other. The locations of the intersections can be seen in the map on lower left corner.

analysis of the deep reflection seismic profile 9HR (for location, see Figure 15). We correlate these characteristic features with the Saxothuringian terrane. To the south across the Bohemian massif and Molasse basin, the Moho dips gently to the south reaching a depth of 37 km. In this area, a ~5-km thick transition zone from the lower crust to Moho was introduced in order to fit PmP amplitudes. No differences between the Barandian and Moldanubian units of the Bohemian massif can be discerned by our seismic results. However, the significant 'floating reflector' at about 20-km depth may be interpreted as a thin zone of magmatic intrusion or a shear zone. Beneath the Molasse basin, the crystalline crust thins. This may be a consequence of the extensional regime that formed the Penninic Ocean [*Roeder*, 1977]. In the Eastern Alps below the Flysch belt and the NCA, the southward dip of the Moho increases abruptly from ~2° to ~4°. Crustal thickness reaches a maximum of 47 km near the PAL at a profile distance of ~450 km. The mantle reflector at ~70-km depth (Figure 7) runs subparallel to this part of the European Moho. Although the nature of this reflector is not clear, we interpret it as a structure related to the general trend of a south-dipping European lithosphere. In the region of south dip, the Moho belongs to the European plate. Farther south, the gently north-dipping Adriatic Moho is separated from the European Moho by a step.

[41] Another large-scale feature in the collision zone is the Sub-Tauern ramp, a crustal-penetrating ramp revealed by the TRANSALP transect [*TRANSALP Working Group*, 2002; *Lüschen et al.*, 2004, 2006]. This ramp is interpreted to be connected to the vertical extrusion of the rocks beneath the TW. We assume that the entire Tauern window was formed by the same tectonic mechanism, and therefore we project the Sub-Tauern ramp into the model for Alp01. At depth, the ramp appears to be tied to the step from European to Adriatic Moho, which is similar to the

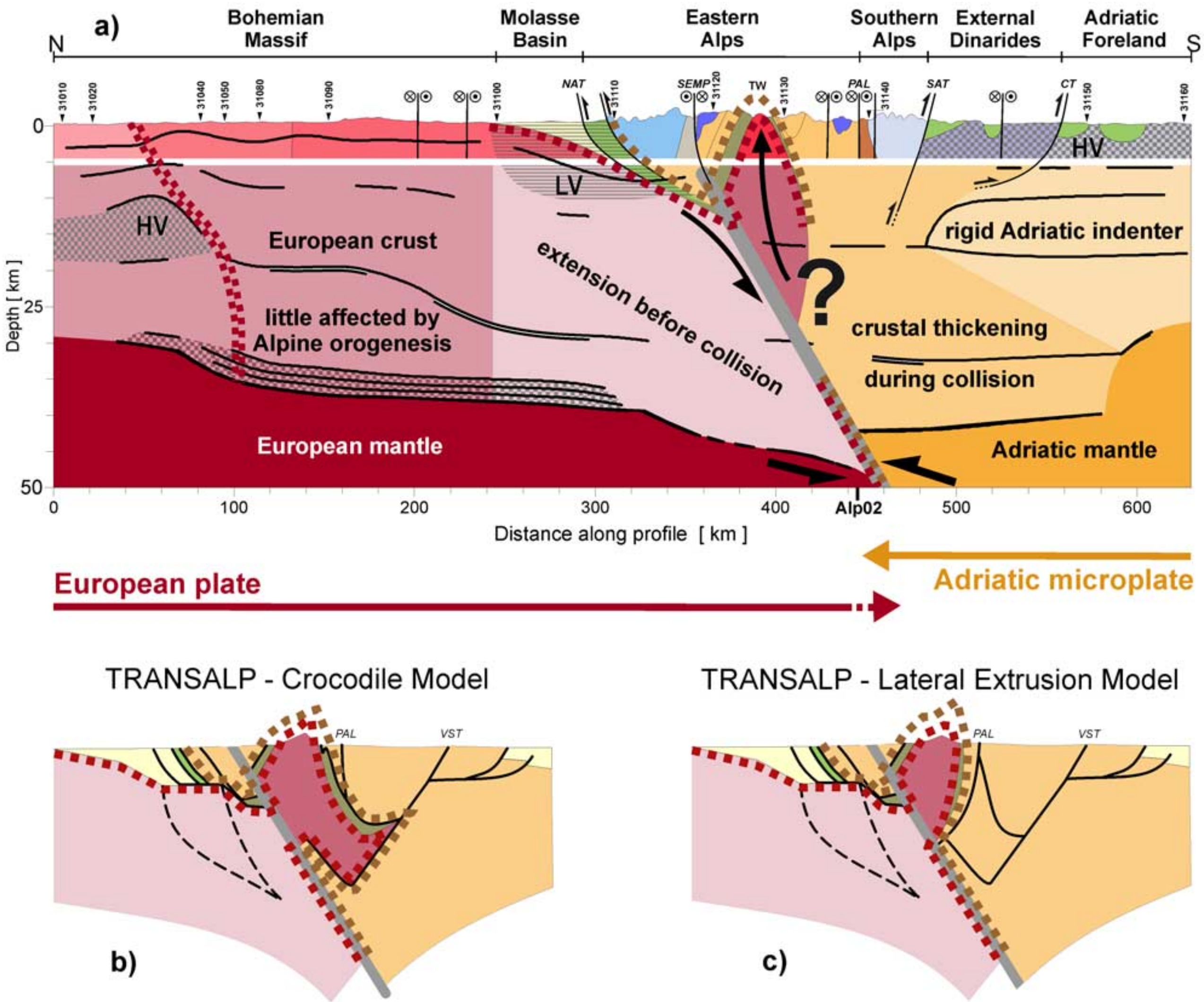


**Figure 16.** (a) Alp01, generalized two-dimensional model of the crust and Moho, geological cross section from Figure 2b (0- to 5-km depth), and tectonic interpretation; normal solid lines show seismic boundary elements verified by reflected or refracted waves; double solid lines are ‘‘floating reflectors’’; areas of relatively high velocity (HV) and low velocity (LV) are marked by specific patterns; bold dotted lines separate Saxothuringian and Moldanubian terranes and European and Adriatic plate; for description of tectonic ,interpretation see text; (b) ‘‘Crocodile Model’’ and (c) ‘‘Extrusion Model’’ for suture between Europe and Adriatic microplate proposed for TRANSALP profile [*TRANSALP Working Group*, 2002].

TRANSALP interpretation. Near the surface, it can be connected to the SEMP, a sinistral strike-slip fault that also shows considerable upward throw of the southern units relative to the northern ones. The apparent dip angle of the Sub-Tauern ramp is 30° along TRANSALP and 24° on Alp01. The difference of apparent dip angle may be caused by the fact that the TRANSALP profile is normal, the Tauern window in its central part, while Alp01 crosses it obliquely near its eastern border. We assume that the extensional character of the European crust north of the Sub-Tauern ramp was not changed by collision. South of the Sub-Tauern ramp, the Tauern window was generated by upward extrusion of Penninic nappes and European crust (gneissic core) along the ramp. The exact mechanism of extrusion, the shape of the extruded fragment of European crust, and therefore the shape of the suture between Europe and Adria-Apulia are not clear at midcrustal levels, even on TRANSALP. Two alternatives were presented by the *TRANSALP Working Group* [2002], the ‘‘Crocodile Model’’ and the ‘‘Lateral Extrusion Model.’’ According to the ‘‘Crocodile Model,’’ the edge of the Tauern window crust wedges about 50 km deep into the Adriatic microplate splitting-up its upper and lower crust. The ‘‘Lateral Extrusion Model’’ describes the Eastern Alps in an indenter style. Parts of the Southern Alps are considered as a rigid block enforcing vertical and lateral extrusion of the Tauern window. Both models explain the more than 25 km exhumation of the Tauern window [*Fügenschuh et al.*, 1977] and are also consistent with our Alp01 seismic velocity model and the major fault systems. The SAT on Alp01 corresponds with the Valsugana thrust on TRANSALP (Figures 16a–16c).

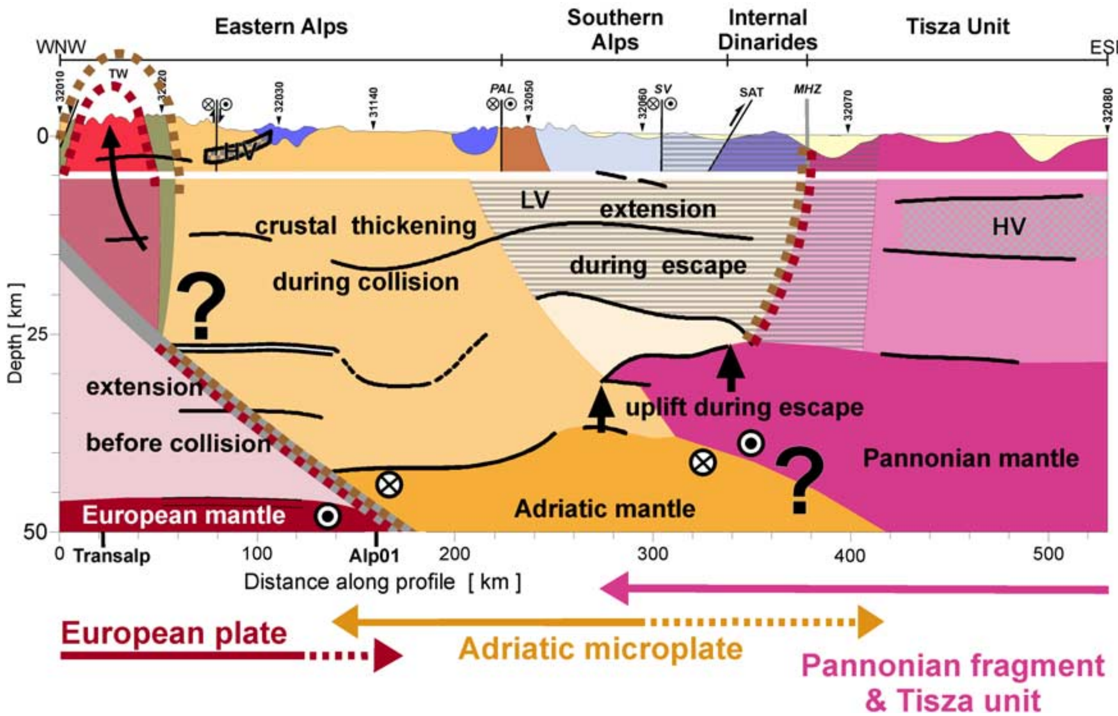


**Figure 17.** Alp02, generalized two-dimensional model of the crust and Moho, geological cross section from Figure 2c (0- to 5-km depth), and tectonic interpretation; bold dotted lines separate European plate, Adriatic microplate, and Tisza unit. For other symbols, see caption for Figure 16.

[42] In the vicinity of the south end of Alp01, the depth of the Adriatic Moho decreases abruptly from ~40 to 28–30 km. We interpret this segment of relatively thin crust as the relatively undeformed Adriatic-Apulian crust. South of profile distance 480 km, we found high velocities in the little to moderately deformed carbonate platform of the External Dinarides and Adriatic foreland and plain and horizontal reflecting horizons in the upper and middle crust. With the help of these indicators, we approximately delineate a block not affected by crustal deformation during collision and correlate it with the "rigid" Adriatic indenter. The Southern Alps and External Dinarides are backthrusted on South Alpine thrust, and Cicaria thrust, and several minor thrust faults that are not shown in Figures 2b and 16. A basal décollement below the External Dinarides is interpreted at ~15-km depth in the LVZ south of 480-km profile distance. Generally, the Adriatic (or South Alpine) indenter is seen as the Adriatic crust south of the PAL indenting toward the north [e.g., *Ratschbacher et al.*, 1991]. The "rigid" Adriatic indenter in our interpretation is restricted to the undeformed crust. South of the Sub-Tauern ramp and north of the "rigid" Adriatic indenter, crustal thickening occurred during collision by mechanisms such as nappe stacking, thrust faulting, and vertical extrusion. Stacking of lower crust is consistent with the "Crocodile" model of the TRANSALP transect [*Lüschen et al.*, 2004], and this mechanism of lower crustal thickening should also be considered along Alp01.

## 8.2. Tectonic Interpretation of the Alp02 Velocity Model

[43] The Alp02 profile provides much new insight about the transition between the Alps and the Pannonian domain (Figure 17). The European Moho cannot be identified uniquely from our seismic data. However, its depth is constrained by the intersecting ALP'75 and TRANSALP profiles. At the profile distance 140 km, the Adriatic Moho begins at a depth of 42 km. The location of the Sub-Tauern ramp can also be inferred from its depth at the intersection of Alp02 with TRANSALP and the location of the step from European to Adriatic Moho. This step in Moho depth at ~130 km along the model is near the intersection with Alp01, where we interpret the European mantle to be underthrusting the Adriatic mantle. On Alp02, we cannot determine the polarity of this underthrusting on the basis of our data; however, we assume the same sense as along Alp01. Because of the orientation of the Alp02 profile, the relative displacement of the European and the Adriatic mantle has its major component normal to the plane of the cross section. The suture between Europe and the Adriatic microplate is constrained by the same criteria as on Alp01, and it has the same uncertainties, especially in the middle crust. The depth extent of anisotropy at the intersection of TRANSALP and Alp02 (Figure 15) down to ~25 km could indicate the depth extent of European crust vertically extruded in the TW. However, the lateral resolution of the TRANSALP model and especially the Alp02 model is too low to clearly distinguish between anisotropy and lateral heterogeneity at these depth levels. A subhorizontal 'floating reflector' at 26-km depth extends from the Sub-Tauern ramp about 80 km into the Adriatic crust without deformation. Because Alp02 strikes obliquely to the Sub-Tauern ramp, the extent of the 'floating reflector' to the south of the ramp may be only 20–30 km. An interpretation could be a postcollision magmatic intrusion (sill) related to the Oligocene intrusives (tonalities) that outcrop nearby

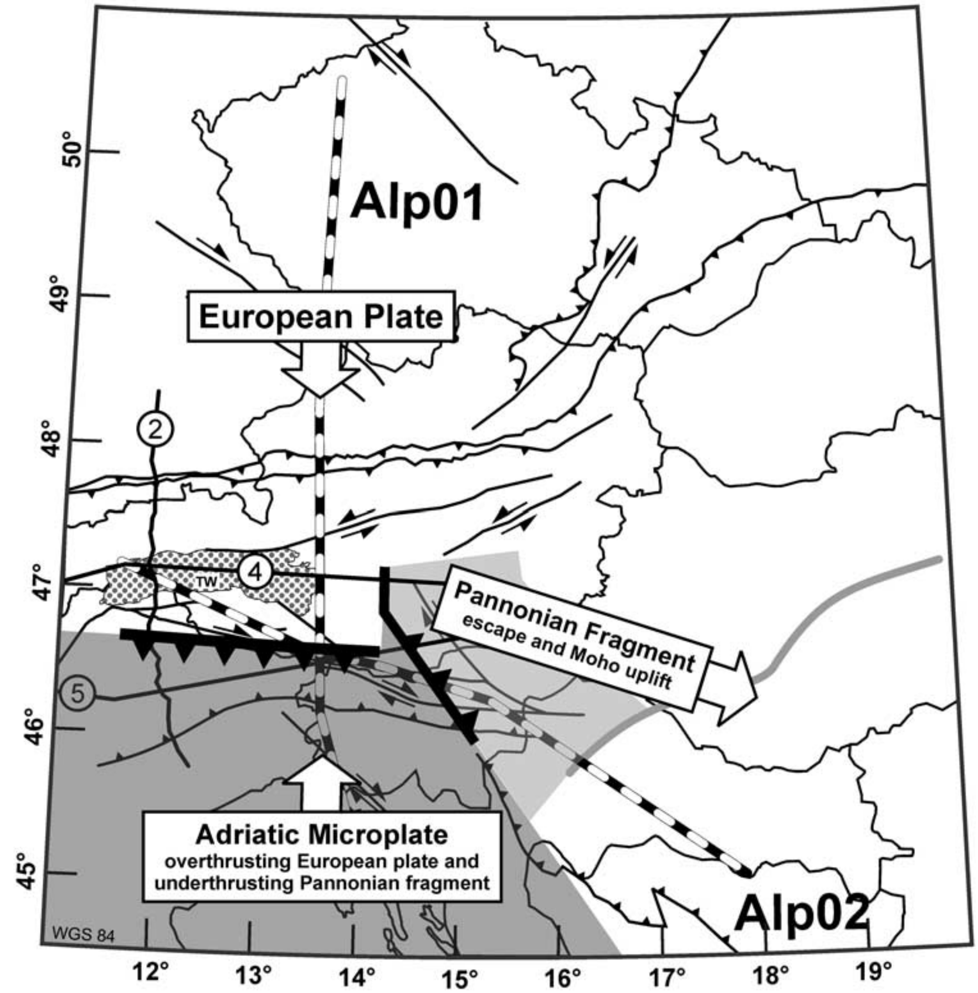


**Figure 18.** Schematic map of the plate tectonic setting of the Eastern Alpine area as derived from Alp01, Alp02, and earlier experiments (2, TRANSALP; 4, ALP'75; 5, Lago-Lagorai>Travisio>East); the northern boundary between the Pannonian fragment and the European plate is not constrained by these data. Big arrows show movement directions.

[*Castellarin et al.*, 2006] (Figure 2a). This interpretation implies that exhumation of the Tauern window, which was most active in the Miocene, did not deform this part of the lower Adriatic crust.

[44] The transition to the Pannonian domain takes place under the western half of the Southern Alps (profile distance ~280 km). At the surface, this transition is manifested by a change to low topography, which is associated with the basins of the Sava depression at the east end of Alp02 (Figures 2a and 2c). At upper and middle crustal levels, we observe low Pg velocities that may be an expression of extensional processes related to escape and the tectonic deformation at the MHZ. Southeast of the MHZ, Pg velocities increase again. The middle crust of the Tisza unit is characterized by higher velocities than the middle crust in the other areas of Alp02.

[45] The most noteworthy feature that accompanies the transition to the Pannonian domain is the ~10-km upward jump of the Moho along the profile at about 280 km (see also Figures 9, 10, and 14). We interpret this sudden decrease of crustal thickness as the manifestation of crustal thinning introduced by the extension associated with the tectonic escape process and its corresponding isostatic compensation since the late Oligocene and early Miocene. Ductile thinning of the lower crust in conjunction with extrusion and escape processes in the Eastern Alps was also assumed by *Ratschbacher et al.* [1991]. Gravimetric studies based on the TRANSALP profile [*Ebbing et al.*, 2006] and a preliminary seismic three-dimensional model for the whole ALP 2002 investigation area [*Brückl et al.*, 2006] suggest that the lithosphere is near isostatic equilibrium in this area. A similar jump in the Moho was found to the ~NNW on ALP'75 and Lago-Lagorai>Tarvisio>East [*Yan and Mechie*, 1989; *Scarascia and Cassinis*, 1997]. *Scarascia and Cassinis* [1997] classified the part of the Moho east of this jump as the "thin Adriatic Moho" in the context of collision between Europe and the Adriatic microplate. We name it the "Pannonian fragment" on the basis of our new tectonic interpretation given below.

[46] In our tectonic interpretation of Alp02, we consider the Pannonian fragment and the adjoining northwest region of the Tisza unit as one tectonic block both for the sake of simplicity and because tectonic processes at the MHZ were not a target in our study. Actually, the Tisza unit acted

differently from the region north of the MHZ during escape [*Csontos and Nagymarosy*, 1998]. Current deformation across the MHZ as detected by GPS is ~0.8 mm/yr for the compressional component. The strike-slip character is not yet detectable [*Grenerczy and Kenyeres*, 2006]. In a paleogeographic sense, the Pannonian fragment was part of the Adriatic microplate before and during collision (up to the Oligocene) and then became an individual block or somehow connected to Tisza unit during the tectonic escape phase according to our interpretation. After the development of the Pannonian fragment, northward convergence further modified the lithosphere. For example, *Linzer et al.* [2002] determined that 80 km of northward postcollision movement of the Adriatic indenter caused ~60 km of shortening in the Eastern Alps nappe system. *Placer* [1999a] determined that 50 km of SW-NE post-Eocene shortening occurred in the External Dinarides and Southern Alps. At present, the N-S convergence rate between Adria and Europe is about 3 mm/year [*Grenerczy and Kenyeres*, 2006]. At least some part of the corresponding shortening of the lithosphere at deeper levels may be due to thrusting of the Adriatic mantle below the mantle of the Pannonian fragment. The northern front of the Adriatic indenter and the Moho jump to the Pannonian fragment are shown in Figure 18, according the results of Alp01, Alp02, and earlier experiments (Eschenlohe>Trieste, Lago-Lagorai>Travisio> East, ALP'75, TRANSALP). The boundary between the Pannonian fragment and the European plate must be north of the ALP'75 profile and is not covered by Alp01, Alp02, or the older profiles. The existence of a Pannonian fragment and its relation to escape and continuing convergence of Europe and Adria can be derived from the step in Moho topography supported by modeling traveltimes only. However, the crocodile structure and the double Moho inferred by amplitude modeling further supports our interpretation, especially the idea of an Adriatic mantle underthrusting the Pannonian fragment since the escape process fully developed.

## 9. Conclusions

[47] Alp01 and Alp02 represent the two main profiles of the ALP 2002 seismic experiment. Seismic cross sections of lithospheric structure have been derived from these data by interactive modeling using ray-tracing techniques and generating synthetic seismograms. Accuracy, resolution, and uncertainties have been analyzed, and comparisons of the results with earlier investigations have been made. Finally, a tectonic interpretation of the seismic cross sections has been presented. The main features of this interpretation are discussed in turn below.

[48] Along Alp01, the European Moho dips regionally to the south and reaches a maximum depth of 47 km below the PAL. The Adriatic Moho continues to the south at significantly shallower depth (42–40 km). This upward jump between the European and Adriatic Mohos and a prominent mantle reflector in the Alpine area, parallel to and 25 km deeper than the European Moho, support the idea of subduction of the European lithosphere below the Adriatic microplate.

[49] The Sub-Tauern ramp was identified on the basis of the TRANSALP seismic reflection profile [*TRANSALP Working Group*, 2002]. It could not be detected directly by modeling either the Alp01 data or the TRANSALP wide-angle data [*Bleibinhaus and Gebrande*, 2006]. However, the Sub-Tauern ramp can be reasonably projected onto the Alp01 and Alp02 tectonic models, considering constraints from Moho topography (step from European to Adriatic Moho) and near surface faults (SEMP). North of the Sub-Tauern ramp, European crust thinned during periods of extension before collision (formation of the Penninic Ocean), and it has kept this character as indicated by decreasing thickness of the crystalline basement from north to south and the presence of low velocities below the Molasse basin and the Eastern Alpine accretionary wedge. To the south of the Sub-Tauern ramp, there is a zone where the Penninic nappes and the European crust (Tauern window) extruded and the Adriatic crust thickened. Below the External Dinarides and the Adriatic foreland, a (more or less) rigid Adriatic indenter can be delineated by high velocities near the surface, planar horizontal reflectors at midcrustal levels, and a normal to shallow Moho (28 km) at the southern end of Alp01.

[50] The most prominent tectonic feature on Alp02 is a jump in Moho depth from ~37 to 27–29 km at the interpreted transition from the Alpine domain to the Pannonian domain. It separates an interpreted Pannonian fragment from the Adriatic microplate. Further along the Alp02, the Moho continues smoothly into the Tisza unit. The Moho jump on Alp02 and the development of the interpreted Pannonian fragment are regarded as a consequence of crustal thinning due to tectonic escape from the Alpine collision area to the unconstrained margin represented by the Pannonian basin since the late Oligocene to early Miocene. This interpretation is further supported by the sudden decrease of surface elevation and an extended area of relatively low crustal velocities below the Internal Dinarides. The Moho jump could also facilitate continuing convergence between Europe and the Adriatic microplate by underthrusting of Adriatic mantle below Pannonian mantle. The Moho jump and the crocodile structure we introduced on the basis of amplitude modeling support this idea.

[51] The European upper and middle crust below the Eastern Alps along Alp01 and Alp02 is not characterized by a LVZ, as observed on the TRANSALP [*Bleibinhaus and Gebrande*, 2006] and other profiles [*Yan and Mechie*, 1989; *Scarascia and Cassinis*, 1997]. Anisotropy may be an explanation to some extent, at least at the intersection of Alp02 and TRANSALP, located in the TW. 'Floating reflectors' indicating thin either high- or low-velocity layers were modeled in some places. However, no high-velocity lower crust (>7 km/s) was found in European plate. A less than 5-km-thick transition zone from the lower crust to the mantle (layered structure or a gradient zone) was delineated under the Barrandian and Moldanubian domains of the Bohemian massif. Relatively high velocities at midcrustal levels were found in Saxothuringian (Alp01) and the Tisza unit (Alp02). Prominent faults like the PAL and SEMP are not imaged by our seismic data. The MHZ is represented by the transition from low crustal velocities because of the escape process to the normal to high velocities within the Tisza unit.

[52] The interpretation of data from the Alp01 and Alp02 profiles provides new insights into collision and escape tectonics in the Eastern Alps. Models of the crustal structure are generally consistent with results from earlier experiments, but Alp01 and Alp02 also covered regions not previously investigated by WAR/R techniques. However, a comprehensive three-dimensional image of the most important crustal structures is still missing. Further interpretation work on other ALP 2002 profiles using interactive ray tracing techniques and three-dimensional approaches using the whole data volume of ALP 2002 simultaneously [*Behm*, 2006; *Behm et al.*, 2007] promises to achieve this goal.

[53] **Acknowledgments.** The ALP 2002 experiment was made possible by the scientific and financial contributions from 11 countries. The main financial support was given by the Austrian Academy of Sciences and the Austrian Science Fund (FWF, P15576). IRIS/PASSCAL is supported by the US National Science Foundation (NSF) and provided the majority (~700) of the instrumentation for this experiment, and most of these instruments were provided through grants to the University of Texas at El Paso (State of Texas Higher Education Coordinating Board, NSF/MRI, and DoD). The participation in the fieldwork by the University of Texas at El Paso was funded by National Science Foundation (EAR and Int) and State of Texas Higher Education Coordinating Board. In Poland, ALP 2002 was supported by the Institute of Geophysics of the Polish Academy of Sciences and Institute of Geophysics University of Warsaw. Scientific conferences in Zakopane 2004 and 2005 were financed by the GEODEV project (contract no. EVK2-CT-2002-90005). Stations along the Alp12/TRANSALP line were provided by the Geophysical Instrument Pool Potsdam. The Czech participation was supported by the Geophysical Institute of the Academy of Sciences and the Ministry of Environment of the Czech Republic (VaV 630/3/02). In Croatia, the project was supported by the Ministry of Science, Education and Sports (project no. 195-1953091-3090) and INA-Industrija nafte, d.d. Further support came also from governmental and scientific institutions in Canada, Denmark, Finland, Hungary, and Slovenia. The successful experiment was made possible by the ambitious and careful work of the ALP 2002 Working Group and its members who are not authors are listed below. We thank G. Fuis and C. Prodehl for their careful review and suggestions that help to improve this manuscript. We further say our thanks Johanna Brückl for compiling geological map and cross sections. Members of ALP 2002 Working Group, not authors: K. Aric, M. Behm, T. Bodoky, W. Chwatal, W. Czuba, E. Gaczyński, H. Gebrande, H. Grassl, Z. Hajnal, S. Harder, S. Hock, V. Hoeck, T. Janik, P. Joergensen, G. Kaip, K. Komminhaho, F. Kohlbeck, K.C. Miller, J. Orešković, K. Posgay, E.-M. Rumpfhuber, C. Schmid, R. Schmöller, C. Snelson, A. Špicák, P. Środa, E. Takács, C. Tomek, C. Ullrich, J. Vozár, F. Weber, M. Wilde-Piórko.

## References

Alpine Explosion Seismology Group (1976), A lithospheric seismic profile along the axis of the Alps, 1975. I: First Results, *Pure Appl. Geophys.*, *114*, 1109–1130.

Aric, K., and R. Gutdeutsch (1987), Geophysical aspects of the crustal structures of the Eastern Alps, in *Geodynamics of the Eastern Alps*, edited by H. W. Fluegel and P. Faupl, Franz Deuticke, pp. 309–360.

Behm, M. (2006), Accuracy and resolution of a 3D seismic model of the Eastern Alps, Ph.D. theses, Vienna University of Technology, 157 pp.

Behm, M., E. Brückl, W. Chwatal, and H. Thybo (2007), Application of stacking techniques to 3D wide-angle reflection and refraction seismic data of the Eastern Alps, *Geophys. J. Int.*, in press.

Beránek, B., and A. Zátopek (1981), Earth's crust structure in Czechoslovakia and central Europe by methods of explosion seismology, in *Geophysical Synthesis in Czechoslovakia*, edited by A. Zátopek, Veda, Bratislava, pp. 253–264.

Beránek, B., and A. M. Zounková (1977), Investigations of the Earth's crust in Czechoslovakia using industrial blasting, *Stud. Geophys. Geod.*, *21*, 273–280.

Bleibinhaus, F. (2003), Entwicklung einer simultanen refraktions- und reflexionsseismischen 3D-Laufzeittomographie mit Anwendung auf tiefenseismische TRANSALP-Weitwinkeldaten aus den Ostalpen. PhD thesis, University of Munich, Faculty of Geosciences, 171 pp, http://edoc.ub.uni-muenchen.de/archive/00001263/.

Bleibinhaus, F., and H. Gebrande (2006), Crustal structure of the Eastern Alps along the TRANSALP profile from wide-angle seismic tomography, *Tectonophysics*, *414*(1–4), 51–69, doi:10.1016/j.tecto.2005.10.028.

Bleibinhaus, F., E. Brückl, and ALP 2002 Working Group (2006), Wide-angle observations of ALP 2002 shots on the TRANSALP profile: Linking the two DSS projects, *Tectonophysics*, *414*(1–4), 71–78, doi:10.1016/j.tecto.2005.10.027.

Bressan, G., A. Snidarcig, and C. Venturini (1998), Present state of tectonic stress of the Friuli area (eastern Southern Alps), *Tectonophysics*, *292*(3–4), 211–227.

Brix, F., and O. Schultz (1993), Erdöl und Erdgas in Österreich, Verlag: Naturhistorisches Museum Wien und F. Berger, Horn, Wien, 688.

Brückl, E., et al. (2003), ALP 2002 Seismic Experiment, *Stud. Geophys. Geod.*, *47*, 671–679.

Brückl, E., U. Mitterbauer, and M. Behm (2006), Studies on crustal structure and gravity in the Eastern Alps, in Geodetic Deformation Monitoring: From Geophysical to Engineering Roles. *IAG Symposium*, *131*, editors F. Sanso and A. J. Gil, 181–192.

Castellarin, A., R. Nicolich, R. Fantoni, L. Cantelli, M. Sella, and L. Selli (2006), Structure of the lithosphere beneath the Eastern Alps (southern sector of the TRANSALP transect), *Tectonophysics*, *414*, 259–282.

Červeny, V., and I. Pšenčik (1983), SEIS83—Numerical modelling of seismic wave fields in 2-D laterally varying layered structures by the ray method, in Documentation of Earthquake Algorithms, edited by E. R. Engdal, Rep. SE-35, World Data Center for Solid Earth Geophysics, Boulder, Colo., 36-40.

Csontos, L., and A. Nagymarosy (1998), The Mid-Hungarian line: A zone of repeated tectonic inversions, *Tectonophysics*, *297*, 51–71.

Dallmeyer, D., W. Franke, and K. Weber (1994), *Pre-Permian Geology of Central and Eastern Europe*, Springer, New York.

Dèzes, P., and P. A. Ziegler (2001), European Map of the Mohorovicic discontinuity, 2nd EUCOR-URGENT Workshop (Upper Rhine Graben Evolution and Neotectonics), Mt. St. Odile, Franc.

Doglioni, C., and A. Bosellini (1987), Eoalpine and Mesoalpine tectonics in the Southern Alps, *Geol. Rundsch.*, *76/3*, 735–754.

Ebbing, J., C. Braitenberg, and H.-J. Götze (2006), The lithospheric density structure of the Eastern Alps, *Tectonophysics*, *414*, 145–155.

Fodor, L., B. Jelen, E. Marton, D. Skaberne, J. Čar, and M. Vrabec (1998), Miocene-Pliocene tectonic evolution of the Slovenian Periadriatic line and surrounding area—Implication for Alpine-Carpathian extrusion models, *Tectonics*, *17*, 690–709.

Franke, W., and A. Żelaźniewicz (2000), The eastern termination of the Variscides: terrane correlation and kinematic evolution, in: Orogenic processes: quantification and modelling in the Variscan Belt, edited by W. Franke, W. Haak, O. Oncken, and D. Tanner, *Geological Society, London, Special Publications,* vol. 179, pp. 63–85.

Fügenschuh, B., D. Seward, and N. Mancktelow (1977), Exhumation in a convergent orogen: The western Tauern window, *Terra Nova*, *9*, 213–217.

Giese, P., and C. Prodehl (1976), Main features of crustal structure in the Alps, in Explosion seismology in Central Europe, edited by P. Giese and C. Prodehl, pp. 347–375, Springer, New York.

Grad, M., et al. (2003), Crustal structure of the Trans-European suture zone region along POLONAISE'97 seismic profile P4, *J. Geophys. Res.*, *108*(B11), 2541, doi:10.1029/2003JB002426.

Grad, M., A. Guterch, G. R. Keller, T. Janik, E. Hegedüs, J. Vozár, A. Ślaczka, T. Tiira, and J. Yliniemi (2006), Lithospheric structure beneath trans-Carpathian transect from Precambrian platform to Pannonian basin—CELEBRATION 2000 seismic profile CEL05, *J. Geophys. Res.*, *111*, B03301, doi:10.1029/2005JB003647.

Grenerczy, G., and A. Kenyeres (2006), Crustal deformation between Adria and the European platform from space geodesy, in: *The Adria microplate: GPS geodesy, tectonics and hazards*, edited by N. Pinter, G. Grenerczy, J. Weber, S. Stein, and D. Medak, *NATO Science Series IV: Earth and Environmental Sciences, 61*, 321–334.

Guterch, A., M. Grad, H. Thybo, and G. R. Keller (1999), POLONAISE'97: International seismic experiment between Precambrian and Variscan Europe in Poland, *Tectonophysics*, *314*, 101–121.

Guterch, A., M. Grad, A. Špićák, E. Brueckl, G. R. Keller, and H. Thybo (2003a), An overview of recent seismic refraction experiments in Central Europe, *Stud. Geophys. Geod.*, *47*, 651–657.

Guterch, A., M. Grad, G. R. Keller, K. Posgay, J. Vozar, A. Špićák, E. Brueckl, Z. Hajnal, H. Thybo, and O. Selvi (2003b), CELEBRATION 2000 Seismic Experiment, *Stud. Geophys. Geod.*, *47*, 659–669.

Hatcher, R., and R. T. Williams (1986), Mechanical model for single thrust sheets, *GSA Bull.*, *97*, 975–985.

Höggerl, N. (1989), Rezente Höhenänderungen in Österreich abgeleitet aus Präzisionsnivellement-Messungen, *Österreichische Beiträge zu Meteorologie und Geophysik*, *2*, 161–173.

Hole, J. A. (1992), Nonlinear high-resolution three-dimensional seismic travel time tomography, *J. Geophys. Res.*, *97*, 6553–6562.

Hrubcová, P., P. Sroda, A. Špićák, A. Guterch, M. Grad, G. R. Keller, E. Brueckl, and H. Thybo (2005), Crustal and uppermost mantle structure

of the Bohemian massif based on CELEBRATION 2000 data, *J. Geophys. Res.*, *110*, B11305, doi:10.1029/2004JB003080.
Janik, T., J. Yliniemi, M. Grad, H. Thybo, and T. Tiira (2002), Crustal structure across the TESZ along POLONAISE'97 seismic profile P2 in NW Poland, *Tectonophysics*, *360*, 129–152.
Joksović, P., and B. Andrić (1982), Report on examination of earth crust composition by deep seismic sounding on the profile of Dugi otok—Virovitica, Expert Document Fund, Geofizika, Zagreb.
Joksović, P., and B. Andrić (1983), Report on examination of earth crust composition by deep seismic sounding on the profile of Pula—Maribor, Expert Document Fund, Geofizika, Zagreb.
Komminaho, K. (1997), Software manual for programs MODEL and XRAYS—A graphical interface for SEIS83 program package, Rep. No. 20, 31, Department of Geophysics, University of Oulu.
Linzer, H.-G., K. Decker, H. Pereson, R. Dell'Mour, and W. Frisch (2002), Balancing lateral orogenic float of the Eastern Alps, *Tectonophysics*, *354*, 211–237.
Lippitsch, R., E. Kissling, and J. Ansorge (2003), Upper mantle structure beneath the Alpine orogen from high-resolution teleseismic tomography, *J. Geophys. Res.*, *108*(B8), 2376, doi:10.1029/2002JB002016.
Lüschen, E., B. Lammer, H. Gebrande, K. Millahn, and R. Nicolich (2004), Orogenic structure of the Eastern Alps, Europe, from TRANSALP deep seismic reflection profiling, *Tectonophysics*, *388*, 85–102.
Lüschen, E., D. Borrini, H. Gebrande, B. Lammer, K. Millahn, F. Neubauer, and R. Nicolich (2006), TRANSALP_deep crustal Vibroseis and explosive seismic profiling in the Eastern Alps, *Tectonophysics*, *414*(1–4), 9–38.
Majdański, M., M. Grad, and A. Guterch (2006), 2-D seismic tomographic and ray tracing modelling of the crustal structure across the Sudetes Mountains basing on SUDETES 2003 experiment data, *Tectonophysics*, *413*(3–4), 49–269.
Mancktelow, N., D. Stockli, B. Grollimund, W. Müller, and B. Fügenschuh (2001), The DAV and Periadriatic fault system in the Eastern Alps south of the Tauern window, *Int. J. Earth Sci.*, *90*, 593–622.
Matte, P. (2001), The Variscan collage and orogeny (480–290 Ma) and the tectonic definition of the Armorica microplate: A review, *Terra Nova*, *13*, 122–128.
Miller, H., H. Gebrande, and E. Schmedes (1977), Ein verbessertes Strukturmodell für die Ostalpen, abgeleitet aus refraktionsseismischen Daten unter Berücksichtigung des Alpenlängsprofils, *Geol. Rundsch.*, *66*, 289–308.
Moores, E. M., and R. J. Twiss (1995), *Tectonics*, W.H. Freeman, New York, 415.
Oberhauser, R. (1980), Der Geologische Aufbau Österreichs, Springer, New York, 699 pp.
Pamić, J., B. Tomljenović, and D. Balen (2002a), Geodynamic and petrogenetic evolution of Alpine ophiolites from the central and NW Dinarides: an overview, *Lithos*, *6*(2005.5), 113–142.
Pamić, J., D. Balen, and M. Herak (2002b), Origin and geodynamic evolution of Late Paleogene magmatic associations along the Periadriatic-Sava-Vardar magmatic belt, *Geodinamica Acta*, *15*(4), 209–231.
Peresson, H., and K. Decker (1997), Far-field effects of Late Miocene subduction in the Eastern Carpathians: E–W compression and inversion of structures in the Alpine– Carpathian– Pannonian region, *Tectonics*, *16*(1), 38–56.
Pitra, P., J. B. Burg, and M. Guiraud (1999), Late Variscan strike-slip tectonics between the Tepla-Barrandian and Moldanubian terranes (Czech Bohemian massif): Petrostructural evidence, *J. Geol. Soc. London*, *156*, 1003–1020.
Placer, L. (1996), Displacement along the Sava fault, *Geologija*, *39*, 283–287.
Placer, L. (1999a), Contribution to the macrotectonic subdivision of the border region between Southern Alps and External Dinarides, *Geologija*, *41*, 223–255.
Placer, L. (1999b), Structural meaning of the Sava folds, *Geologija*, *41*, 191–221.
Poljak, M. (2000), Structural-tectonic map of Slovenia 1: 250.000, Geological Survey of Slovenia.
Poljak, M., M. Zivčić, and P. Zupančič (2000), The seismotectonic characteristics of Slovenia, *Pure Appl. Geophys.*, *157*, 37–55.
Ratschbacher, L., W. Frisch, H. G. Linzer, and O. Merle (1991), Lateral extrusion in the Eastern Alps, Part 2.: Structural analysis, *Tectonics*, *10*(2), 257–271.
Reinecker, J., and W. A. Q. Lenhardt (1999), Present-day stress field and deformation in eastern Austria, *Int. J. Earth Sci.*, *88*, 532–550.
Roeder, D. (1977), Continental convergence in the Alps, *Tectonophysics*, *40*, 339–350.
Royden, L. H., F. Horvath, and J. Rumpler (1983), Evolution of the Pannonian basin system: 1. Tectonics, *Tectonics*, *2*, 63–90.
Saftić, B., J. Velić, O. Sztano, G. Juhasz, and Ivković (2003), Tertiary subsurface facies, source rocks and hydrocarbon reservoirs in the SW part of the Pannonian basin (Northern Croatia and Southwestern Hungary), *Geol. Croat.*, *56*, 101–122.
Scarascia, S., and R. Cassinis (1997), Crustal structures in the central-eastern Alpine sector: A revision of available DSS data, *Tectonophysics*, *271*, 157–188.
Schmid, S., B. Fügenschuh, E. Kissling, and R. Schuster (2004), Tectonic map and overall architecture of the Alpine orogen, *Swiss J. Geosci.*, *07*(1), 93–117.
Środa, P. (1999), Modifications of software package ZPLOT by C. Zelt, Inst. Geophys., Pol. Acad. Sc., Warsaw.
Tomek, C., V. Dvořáková, and S. Vrána (1997), Geological interpretation of the 9HR and 503 M seismic profiles in western Bohemia, *J. Geol. Sci. Prague*, *47*, 43–51.
Tomljenović, B., and L. Csontos (2001), Neogene-Quaternary structures in the border zone between Alps, Dinarides and Pannonian basin (Hrvatsko Zagorje and Karlovac basins, Croatia), *Int. J. Earth Sci.*, *90*, 560–578.
TRANSALP Working Group (2002), First deep seismic reflection images of the Eastern Alps reveal giant crustal wedges and transcrustal ramps, *Geophys. Res. Lett.*, *29*(10), 1452, doi:10.1029/2002GL014911.
Vrabec, M., and L. Fodor (2006), Late Cenozoic tectonics of Slovenia: Structural styles at the northeastern corner of the Adriatic microplate, in The Adria microplate: GPS Geodesy, tectonics and hazards, edited by N. Pinter et al., *NATO Science Series IV: Earth and Environmental Sciences*, vol. 61, 413.
Vrána, S., and V. Štědrá (1998), Crustal structure of the western part of the Bohemian massif, Czech Republik, *Episodes*, *21*(4), 241–247.
Yan, Q. Z., and J. Mechie (1989), A fine structural section through the crust and lower lithosphere of the Alps, *Geophys. J.*, *98*, 465–488.
Zelt, C. (1994), ZPLOT-An interactive plotting and picking program for seismic refraction data. Bullard Lab., Univ. of Cambridge, Cambridge, UK.
Zupančič, P., I. Cecič, A. Gosar, L. Placer, M. Poljak, and M. Živčić (2001), The earthquake of 12 April 1998 in the Krn Mountains (Upper Soèa Valley, Slovenia) and its seismotectonic characteristics, Ljubljana, *Geologija*, *44/1*, 169–192.

---

F. Bleibinhaus and E. Brückl, Institute of Geodesy and Geophysics, Vienna University of Technology, Vienna, Austria. (ebrueckl@mail.tuwien.ac.at)

A. Gosar, Environmental Agency of Slovenia and Faculty of Natural Sciences and Engineering, University of Ljubljana, Ljubljana, Slovenia.

M. Grad and M. Majdański, Institute of Geophysics, University of Warsaw, Warsaw, Poland.

A. Guterch, Institute of Geophysics, Polish Academy of Sciences, Warsaw, Poland.

E. Hegedűs, Eötvös Loránd Geophysical Institute, Budapest, Hungary.

P. Hrubcová, Geophysical Institute, Academy of Sciences of the Czech Republic, Prague, Czech Republic.

G. R. Keller, Department of Geological Sciences, University of Texas at El Paso, El Paso, USA.

F. Šumanovac, Faculty of Mining, Geology and Petroleum Engineering, University of Zagreb, Zagreb, Croatia.

T. Tiira, Institute of Seismology, University of Helsinki, Helsinki, Finland.

H. Thybo, Geological Institute, University of Copenhagen, Copenhagen, Denmark.

J. Yliniemi, Sodankylä Geophysical Observatory, University of Oulu, Oulu, Finland.